electronic design

THE AUTHORITY ON
EMERGING TECHNOLOGIES
FOR DESIGN SOLUTIONS

September 2015 electronicdesign.com

$10.00 Powered by Penton

Periodicals Postage Paid • USPS 100 Approved Poly

electronic design

THE AUTHORITY ON
EMERGING TECHNOLOGIES
FOR DESIGN SOLUTIONS

September 2015 electronicdesign.com

the ULTIMATE WEARABLE

p| 14

$10.00 Powered by Penton

Periodicals Postage Paid • USPS 100 Approved Poly

September 2015 VOLUME 63, ISSUE 9

electronic design

InThisIssue

FEATURES

14


12

36
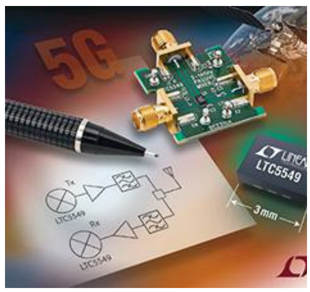

20
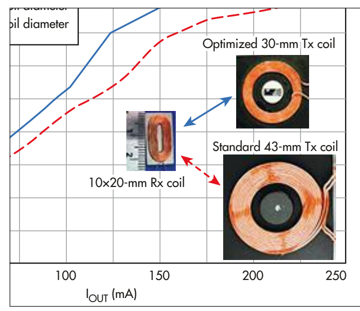

NEWS & ANALYSIS

IDEAS FOR DESIGN

COLUMNS & DEPARTMENTS


26

28


EDITORIAL MISSION:
To provide the most current, accurate, and in-depth technical coverage of the key emerging technologies that engineers need to design tomorrow's products today.

ELECTRONIC DESIGN (ISSN 0013-4872) is published monthly by Penton Media Inc., 9800 Metcalf Ave., Overland Park, KS 66212-2216. Paid rates for a one-year subscription are as follows: $120 U.S., $180 Canada, $240 International. Periodicals postage paid at Kansas City, MO, and additional mailing offices. Editorial and advertising addresses: ELECTRONIC DESIGN, 1166 Avenue of the Americas, New York, NY 10036. Telephone (212) 204-4200. Printed in U.S.A. Title registered in U.S. Patent Office. For subscriber services or to order single copies, write to Electronic Design, PO Box 2100, Skokie, IL 60076. POSTMASTER: Send change of address to Electronic Design, PO Box 2100, Skokie, IL 60076. Canadian Post Publications Mail agreement No. 40612608. Canada return address: IMEX Global Solutions, P.O. Box 25542, London, ON N6C 6B2.

on electronicdesign.com

THE DIFFERENCE BETWEEN SON, C-RAN, AND HETNET

http://electronicdesign.com/communications/what-s-difference-between-son-c-ran-and-hetnet

Get ready for next-generation mobile wireless by gaining an understanding of SON, C-RAN, and HetNet technologies.

blogs

LOUIS FRENZEL
COMMUNICATIONS

- Ranking the Top 5 Wireless Devices

BILL WONG
EMBEDDED/SYSTEMS/SOFTWARE

- Securing the Internet of Things

PATRICK MANNION
TEST & MEASUREMENT

- Why Is the USB Type-C Connector So Testy?

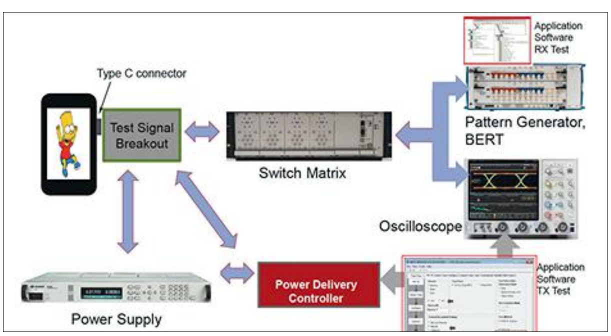

CONFIGURE A CAR WITH SMARTWATCH APPLICATIONS

http://electronicdesign.com/iot/configure-car-smart-watch-applications

A smartwatch may be a perfect tool for car customization, since it saves driver's preferences and can share them with all of your connected devices.

GALLERY: THE LATEST IN OSCILLOSCOPES

http://electronicdesign.com/test-measurement/gallery-6-digital-oscilloscopes-tackling-high-speed-communications-signals

In this image gallery, we provide an overview of the latest digital oscilloscopes for testing complex RF communications, ranging from current standards to 5G technologies.

SMART-CAMERA PROCESSING CHOICES

http://electronicdesign.com/microprocessors/apus-vs-fpgas-battle-smart-camera-processing-supremacy

Smart cameras based on x86 are optimized for increasingly sophisticated tasks that can enhance productivity, precision, and security for a wide range of applications.

join us online

Follow us on Facebook: www.facebook.com/ElectronicDesign
and Twitter: www.twitter.com/ElectronicDesgn

WIN YOUR DREAM BENCH
$141,000 of instruments and software†
www.keysight.com/find/DreamBench

Touch. Discover. Solve.

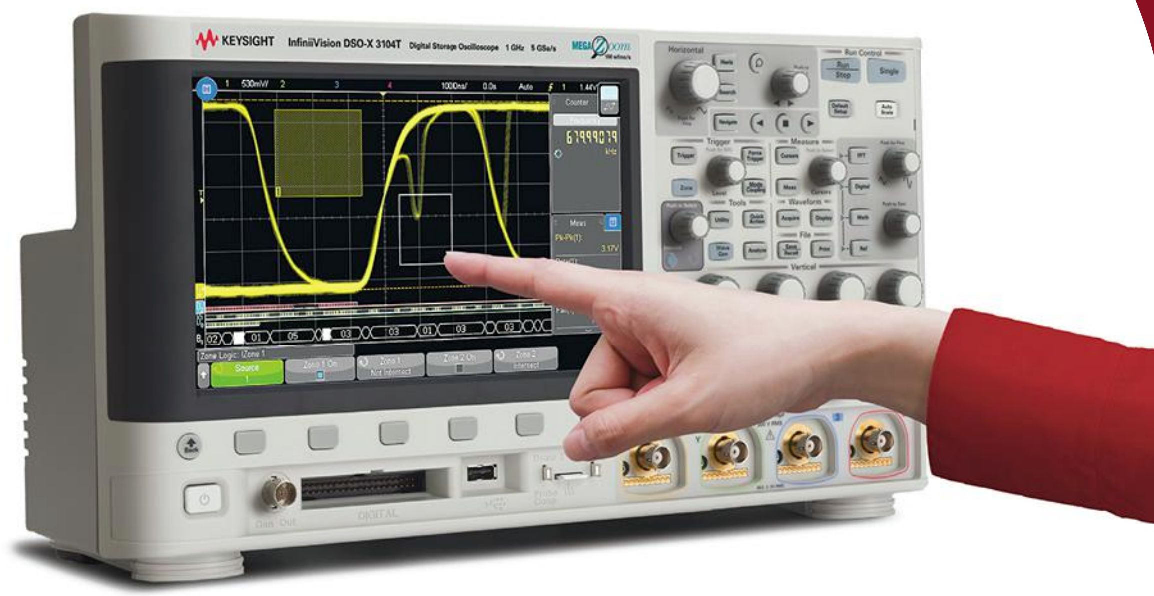

Oscilloscopes redefined.

We've improved on the proven. The new Keysight 3000T oscilloscope is the next-generation of the InfiniiVision X-Series. With its zone touch triggering, you can trigger on any signal in just two steps. So you can isolate a signal in seconds—much faster than with any competing scope. The 3000T is also a 6-in-1 instrument. Along with your oscilloscope, you can get an MSO, WaveGen function generator, protocol analyzer, DVM and counter. Get in touch with the future of scopes. Take the Trigger Challenge today.

Models	Keysight 3000T X-Series*	Leading Competitor**
Bandwidth	100 MHz-1 GHz	100 MHz-1 GHz
Update Rate	Uncompromised 1M wfms/s	Up to 280K wfms/s
Touch Screen	8.5-inch Capacitive	No
Zone Touch Triggering	Yes	No
Sample Rate	5 GSa/s	2.5 GSa/s (>= 500 MHz) 5 GSa/s (1 GHz)

Newark element14

Take the Trigger Challenge and enter to win a free 3000T at:
www.newark.com/Keysight_Scopes
Buy from an Authorized Distributor 800 463 9275

KEYSIGHT TECHNOLOGIES
Unlocking Measurement Insights

 †Value in USD. See website for full details.
* Refer to Keysight document 5992-0140EN for product specs, and 5989-7885EN for update rate measurements.
** Competitive oscilloscopes are from Tektronix publication 48W-30020-3

Agilent's Electronic Measurement Group is now **Keysight Technologies.**

electronic design
A Penton® Publication
SEPTEMBER 2015

EDITORIAL

CONTENT DIRECTOR: **NANCY K. FRIEDRICH** nancy.friedrich@penton.com
CONTENT PRODUCTION DIRECTOR: **MICHAEL BROWNE** michael.browne@penton.com
CONTENT PRODUCTION SPECIALIST: **ROGER ENGELKE** roger.engelke@penton.com
PRODUCTION EDITOR: **JEREMY COHEN** jeremy.cohen@penton.com
DISTRIBUTION: **VICTORIA FRAZA KICKHAM** SourceESBeditor@penton.com
EMBEDDED/SYSTEMS/SOFTWARE: **WILLIAM WONG** bill.wong@penton.com
CONTENT OPTIMIZATION SPECIALIST: **ILIZA SOKOL** iliza.sokol@penton.com
ASSOCIATE CONTENT PRODUCER: **LEAH SCULLY** leah.scully@penton.com
ASSOCIATE CONTENT PRODUCER: **JAMES MORRA** james.morra@penton.com
CONTRIBUTING EDITOR: **LOUIS E. FRENZEL** lou.frenzel@penton.com

ART DEPARTMENT

GROUP DESIGN DIRECTOR: **ANTHONY VITOLO** tony.vitolo@penton.com
SENIOR ARTIST: **JIM MILLER** jim.miller@penton.com
CONTRIBUTING ART DIRECTOR: **RANDALL L. RUBENKING** randall.rubenking@penton.com

PRODUCTION

GROUP PRODUCTION MANAGER: **CAREY SWEETEN** carey.sweeten@penton.com
PRODUCTION MANAGER: **JULIE GILPIN** julie.gilpin@penton.com

AUDIENCE MARKETING

USER MARKETING DIRECTOR: **BRENDA ROODE** brenda.roode@penton.com
USER MARKETING MANAGER: **DEBBIE BRADY** debbie.brady@penton.com
FREE SUBSCRIPTION/STATUS OF SUBSCRIPTION/ADDRESS CHANGE/MISSING BACK ISSUES
T | 866.505.7173 **F** | 847.763.9673 electronicdesign@halldata.com

SALES & MARKETING

MANAGING DIRECTOR: **TRACY SMITH** **T** | 913.967.1324 **F** | 913.514.6881 tracy.smith@penton.com

REGIONAL SALES REPRESENTATIVES
AZ, NM, TX: **GREGORY MONTGOMERY** **T** | 480.254.5540 gregory.montgomery@penton.com
AK, CA, CO, ID, MT, ND, NV, OR, SD, UT, WA, WI, WY, W/CANADA: **JAMIE ALLEN** **T** | 415.608.1959 **F** | 913.514.3667 jamie.allen@penton.com
AL, AR, IA, IL, IN, KS, KY, LA, MI, MN, MO, MS, NE, OH, OK, TN: **PAUL MILNAMOW** **T** | 312.840.8462 paul.milnamow@penton.com
CT, DE, FL, GA, MA, MD, ME, NC, NH, NJ, NY, RI, PA, SC, VA, VT, WV, EASTERN CANADA: **SHANNON ALO-MENDOSA** **T** | 978.501.7303 Shannon.alo-mendosa@penton.com

INTERNATIONAL SALES
GERMANY, AUSTRIA, SWITZERLAND: **CHRISTIAN HOELSCHER** **T** | 011.49.89.95002778 christian.hoelscher@husonmedia.com
BELGIUM, NETHERLANDS, LUXEMBURG UNITED KINGDOM, SCANDINAVIA, FRANCE, SPAIN, PORTUGAL: **JAMES RHOADES-BROWN** **T** | +011 44 1932 564999 **M** | +011 44 1932 564998 james.rhoadesbrown@husonmedia.com
PAN-ASIA: **HELEN LAI** **T** | 886 2-2727 7799 helen@twoway-com.com

PLEASE SEND INSERTION ORDERS TO: orders@penton.com
PENTON REPRINTS: **WRIGHT'S MEDIA** **T** | 877.652.5295 penton@wrightsmedia.com
CIRCULATION: **CUSTOMER SERVICE** **T** | 866.505.7173 **F** | 847.763.9673 electronicdesign@halldata.com

LIST RENTALS:
SMARTREACH CLIENT SERVICES MANAGER: **DAVID SICKLES** **T** | (212) 204 4379 david.sickles@penton.com

ONLINE

PRODUCT DEVELOPMENT DIRECTOR **RYAN MALEC** ryan.malec@penton.com

DESIGN ENGINEERING & SOURCING GROUP

VICE PRESIDENT & MARKET LEADER: **BILL BAUMANN**
EXECUTIVE DIRECTOR OF CONTENT AND USER ENGAGEMENT: **NANCY K. FRIEDRICH**
GROUP DIRECTOR OF OPERATIONS: **CHRISTINA CAVANO**
GROUP DIRECTOR OF MARKETING: **JANE COOPER**

PENTON

CHIEF EXECUTIVE OFFICER: **DAVID KIESELSTEIN** david.kieselstein@penton.com
CHIEF FINANCIAL OFFICER: **NICOLA ALLAIS** nicola.allais@penton.com
SENIOR VP, DESIGN ENGINEERING GROUP: **PAUL MILLER** paul.miller@penton.com
1166 AVENUE OF THE AMERICAS, 10TH FLOOR
NEW YORK, NY 10036 **T** | 212.204.4200

Penton

Electronic Design | Machine Design | Microwaves & RF | Medical Design | Source ESB | Hydraulics & Pneumatics | Global Purchasing | Distribution Resource | Power Electronics | Defense Electronics | Electronic Design Europe | Engineering TV

MPS®
Simple, Easy Solutions

High Performance ≠ High Price
Call MPS!

Premium DC/DC Power Modules

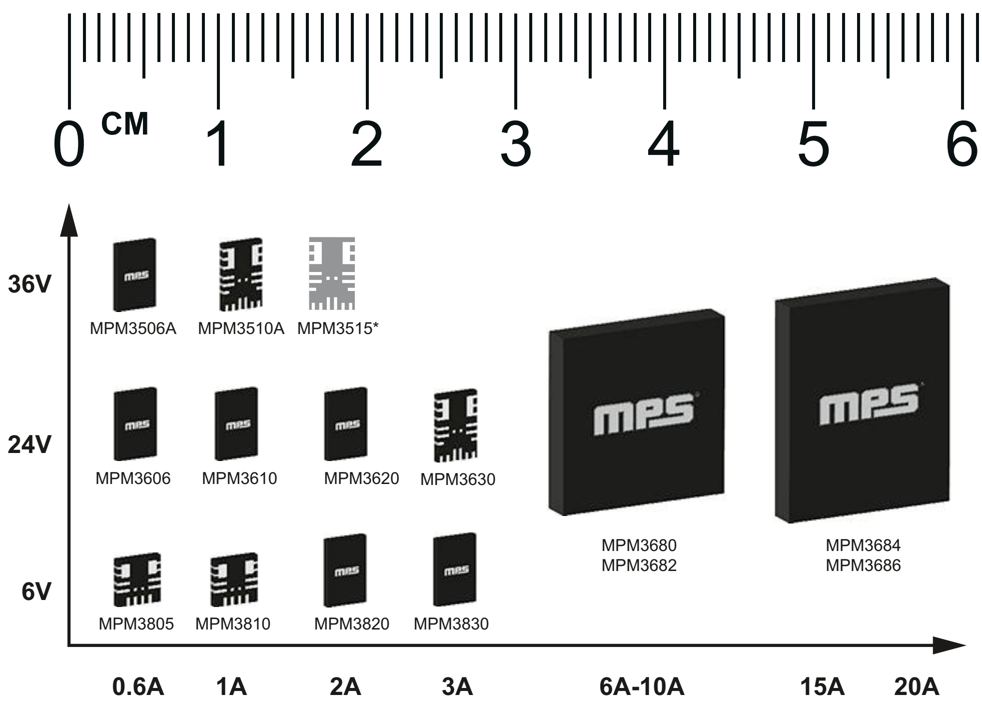

*Coming soon

www.monolithicpower.com

Follow us on:

BILL WONG | Embedded/Systems/Software Editor
bill.wong@penton.com

Flash in the 3D Pan

Storage vendors were showing off their latest wares at the Flash Memory Summit in Santa Clara, Calif. This includes devices like Samsung's 3D, 48-layer V-NAND chip (*Fig. 1a*) that packs in 256 Gbits of 3-bit multi-level-cell (MLC) flash memory. That is 32 Gbytes on a single chip. Not to be outdone, Toshiba's BiCS 48-layer, 3-bit MLC flash chip (*Fig. 1b*) also has 256 Gbits of storage. Samsung's cell uses a 3D Charge Trap Flash (CTF) structure.

Toshiba also announced a 16-layer NAND flash device that uses Through Silicon Via (TSV) technology. This allows the chip to transfer data at rates in excess of 1 Gibt/s. The approach also cuts power requirements in half by reducing core voltage to 1.8 V and I/O to 1.2 V. While the 48-layer devices will provide high capacity, the TSV chips deliver low latency and high bandwidth and the chips have a high IOPS/W.

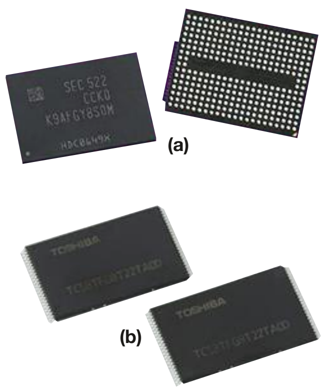

1. Samsung's 3D, 48 layer V-NAND chip (a) packs in 256-Gbits of 3-bit multi-level-cell (MLC) flash memory. Toshiba's 48-layer, BiCS device (b) also uses 3-bit MLC and delivers 256-Gbits of storage.

Riccardo Badalone, CEO and co-founder of Diablo Technologies, kicked off the conference with his keynote, "Disruptive Memory Technology Enables New In-Memory Applications." Of course, he was talking about Diablo Technologies' new DDR4 Memory1 DIMM (*Fig. 2*). Memory1 DIMMs are available with capacities up to 256 Gbytes. That is four times the storage available in DRAM DIMMs and the flash memory is on the memory channel, not the PCI Express bus (*see "Memory Channel Flash Storage Provides Fast RAM Mirroring" on www.electronicdesign.com*).

2. Diablo Technologies' all-flash Memory1 DIMM finds a home in a DDR4 memory slot.

Seagate was touting its PCIe Gen 3, NVMe support with its Nytro XF1440 2.5-in and Nytro XM1440 M.2 SSDs that deliver 25,000 IOPS/W. The hot swappable drives use a SFF-8639 connector and have a maximum capacity of 1.8 Tbytes while the M.2 devices support up to 960 Gybtes. Self-Encrypting Drives (SEDs) are available.

There was discussion of Intel and Micron's XPoint 3D storage and Altera was demonstrating its NAND Flash reference design that can extend the life of flash memory up to 7 times. The reference design used an Arria 10 SoC and implemented Mobiveil's Universal NVM Express Controller (UNEX).

There was never a dull moment at the Flash Memory Summit. ed

News

GRAPHENE-BASED FILM Could Be the Future of Cooling Microelectronics

Due to its high thermal conductivity, graphene-based film has the potential to replace more widely used materials, such as copper and aluminum, for cooling electronic components. This is especially true as manufacturers continue to reduce the size of integrated chips and processors, even as higher data rates push their capabilities to the limit. Now, a Swedish research team from Chalmers University of Technology has developed a method for vastly increasing the cooling properties of graphene-based film, allowing it to more effectively dissipate heat from electronic devices.

The thermal conductivity of graphene-based film can be enhanced by pasting together several layers of the carbon-derived material. But until recently, the number of layers that could be linked, without falling apart, was too low to remove large amounts of heat. By developing a stronger bond between the graphene film and silicon component, the research team was able to increase the thickness of the material. The research team reported that the graphene-based film could now be made with a thickness of 20 micrometers and a thermal conductivity of 1600 W/mk. This is more than four times the thermal conductivity of copper and almost seven times that of aluminum—two of the most commonly used materials in electronic heat sinks.

The research team achieved a higher thermal conductivity by using a process called functionalization, which involves the addition of a property-altering molecule to the material. This was done by adding (3-Aminopropyl) triethoxysilane (APTES) molecules to the graphene film. When heated and put through hydrolysis, the molecule creates silane bonds between the graphene and the electronic component.

The research team noted that such high thermal conductivity would enable graphene-based film to be used in small, high-power applications, including microelectronics, light-emitting diodes (LEDs), and radio frequency components. These devices would also be more sustainable and energy efficient, as less energy will have to be used for cooling purposes. Recent studies have found that almost half the energy required to run computer servers is used for cooling purposes alone.

But graphene-based film is still being studied and, at present, not widely used in electronic devices. In 2012, the graphene market only earned revenues of $9 million. But it is projected that this market will grow significantly over the next 10 years, with a recent report from IDTechEx estimating that the graphene segment will earn revenues of nearly $200 million by 2025. The material is increasingly being used in lithium-ion battery anodes and in the semiconductor market as an alternative to crystalline silicon. ■

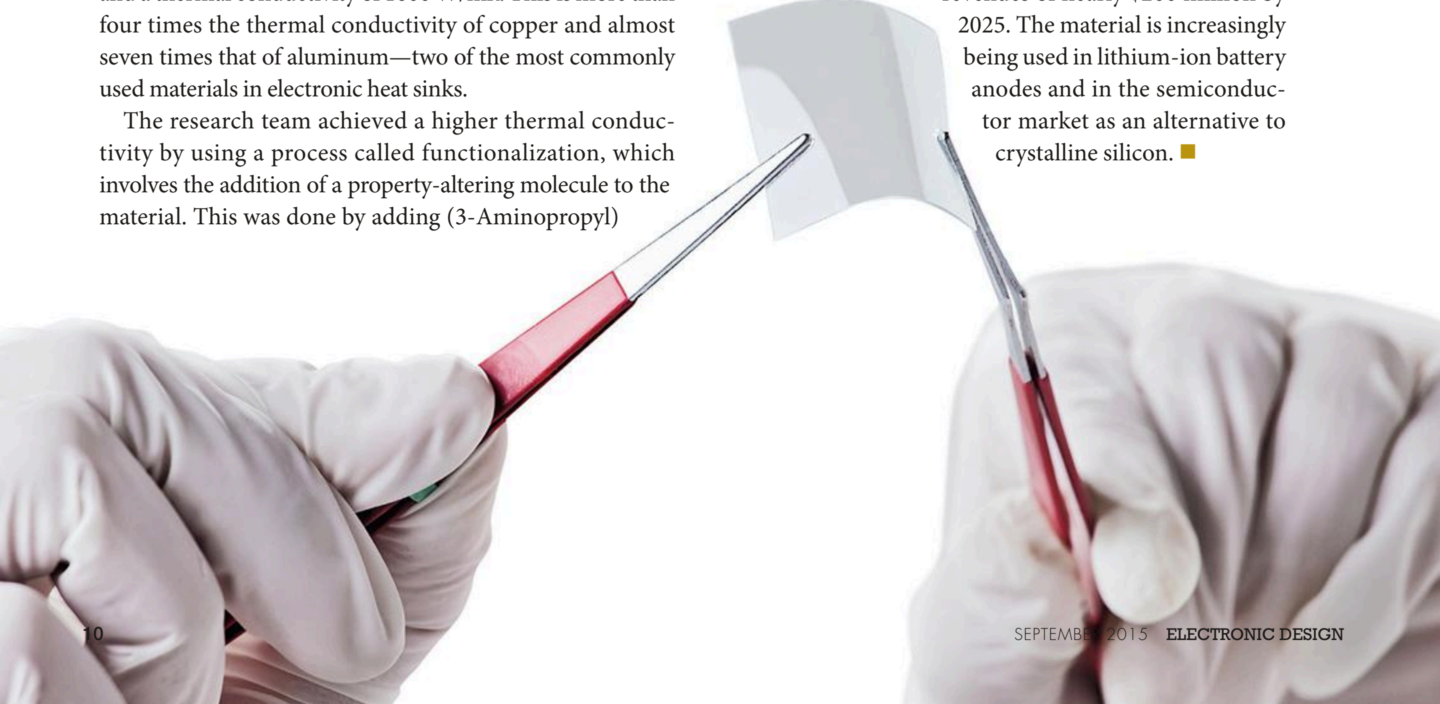

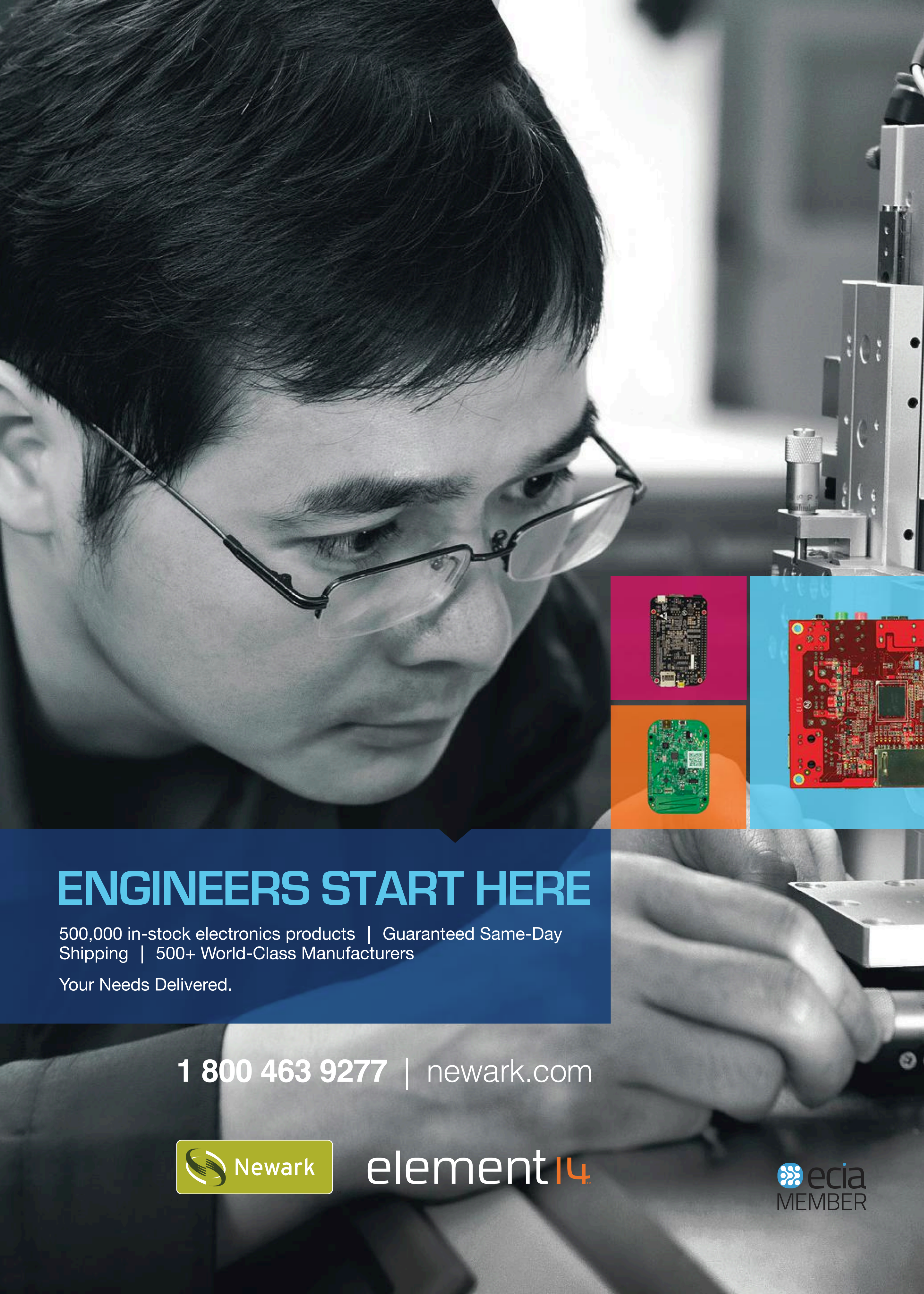

ENGINEERS START HERE
500,000 in-stock electronics products | Guaranteed Same-Day Shipping | 500+ World-Class Manufacturers
Your Needs Delivered.
1 800 463 9277 | newark.com
Newark
element14
ecia MEMBER

IRIS SCANNER UNLOCKS Smartphones Using Infrared LEDs

The growing number of smartphone thefts, both in the United States and abroad, has prompted manufacturers to incorporate more resilient security methods into their designs. Fujitsu Ltd., for instance, recently unveiled the Arrows NX F-04G smartphone, which uses infrared light-emitting diodes (IREDs) to support iris scanning authentication.

The infrared light source, developed by Osram Opto Semiconductors, illuminates the user's eye while a camera simultaneously takes a photograph of the iris. The Oslux SFX 4780S measures only 2.4 in. high and supports a typical radiant intensity of 2900 mW/sr. Using an application called Iris Passport, the smartphone then identifies all of the characteristic features of the iris and unlocks the device. The IRED has a wavelength of 810 nm, which allows the scanner to identify iris patterns for all eye colors. According to Fujitsu Ltd., the entire process will only take half a second to complete.

Such technology is part of a larger movement toward biometric identification methods as users become more vulnerable to theft. A report issued by the Federal Communications Committee in late 2014 found that more than a million smartphone thefts are reported in the United States each year. Because smartphones hold a large amount of personal information, manufacturers are investing in more secure alternatives to four-digit passcode locks and computer backups. ■

CAN THIS NEW Chip Be the Sweet Spot Between NAND and DRAM?

INTEL CORP. AND MICRON TECHNOLOGY HAVE joined forces to introduce a new kind of memory chip to address the explosion of growth in the digital sphere. The technology, called 3D XPoint (pronounced "cross point") is being described as both fast and nonvolatile, meaning that it can serve as either system memory or digital storage. The result, according to Micron CEO Mark Durcan, is the first new memory category to be released since NAND Flash in 1989.

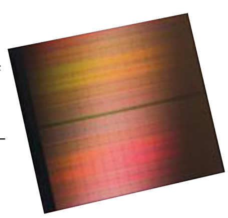

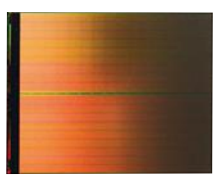

The new technology is a kind of hybrid between dynamic random-access memory (DRAM) and solid-state NAND Flash drives. "It's up to 1,000 times quicker, and writeable in small amounts, so it can be used as memory," said Robert Crooke, senior vice president and general manager of Intel's Non-Volatile Memory Solutions Group. "But it's also nonvolatile, so it can be used as storage." DRAM technology is capable of accessing memory faster than 3D XPoint. Because DRAM is volatile, however, it needs a constant supply of power to save data. In contrast, solid-state NAND Flash is nonvolatile but significantly slower than DRAM and 3D XPoint.

For its part, the 3D XPoint technology is built with thin columns of densely packed memory cells stacked in a three-dimensional crosshatch pattern. The cells intersect across word lines and bit lines, allowing them to be written and accessed individually. According to Micron and Intel, this results in about 1,000 times lower latency than NAND Flash technology, which is forced to erase entire blocks of cells in order to rewrite data. In addition, the technology can be stacked between eight and ten times the density of DRAM chips and will be significantly more durable than NAND Flash, the companies said.

The memory cells, which Intel and Micron both declined to talk about in detail, are written through "bulk material property change." By varying the amount of voltage sent to each selector, the cell changes its physical characteristics to have either high or low electrical resistance, programming the cell to be a zero or a one. According to Crooke, this approach removes the need for transistors in the memory cell—one of the main reasons DRAM technology is so expensive. The cost-per-bit for the new technology, Crooke said, should be somewhere between NAND and DRAM.

The two companies have not revealed much of the underlying architecture behind the 3D XPoint technology, but have said that the technology is targeting programs that have to evaluate large data sets, like gaming, high-fidelity pattern recognition, and the analysis of genomes in medical research. 3D XPoint wafers are currently running in production lines at a joint Micron-Intel facility in Utah.

A release date for the technology has not been announced. ■

WILLIAM WONG | Technical Editor

MEDICAL EXOSKELETONS

IoT-linked assistive limbs give patients mobility.

Today's exoskeletons are a far cry from Marvel's Iron Man, but Tony Stark had the advantage of an arc reactor and almost unlimited power. Iron Man also has powerful servos and armor that gods and aliens have a hard time cracking.

Luckily, practical, wearable exoskeletons are not a cartoon dream. While they are expensive and have significant limitations (such as limited run time), they are nevertheless proving to be invaluable in areas such as medical and industrial applications.

Medical applications include support for rehabilitation and gait training, as well as providing long-term mobility. The Japanese Orthopedic Association (JOA) refers to musculoskeletal disorders as Musculoskeletal Ambulation Disability Symptom Complex, or MADS. This encompasses patients with spinal cord or traumatic brain injuries, cerebrovascular diseases, diseases of the brain, and neuromuscular system problems.

1. Pictured are the offerings from ReWalk Robotics (a) and Ekso Bionics (b).

Become Practical

Exoskeletons have many advantages over other alternatives, like medical scooters (such as the one my father uses). An exoskeleton moves the limbs, allowing the user to stand upright rather than sit. It also enables users to navigate areas like steps that a scooter cannot. Some systems can also allow paraplegic users to walk. Of course, a scooter tends to be more power-efficient and it can incorporate a significantly larger battery. They are also much less expensive than the current crop of exoskeletons.

Many medical exoskeleton platforms are part of the medical Internet of Things (IoT), with wireless communication used to do everything from monitoring a user's progress to configuring the capabilities and operation of the exoskeleton. Many systems allow this to be done with a smartphone or tablet.

Part of the system design challenge is to provide support for doctors and therapists, as well as users. Some systems will be employed in a rehabilitation setting, while others will be used for personal mobility augmenting or replacing wheelchairs or other devices.

ReWalk Robotics' ReWalk Personal System *(Fig. 1a)*, Ekso Bionics' Ekso *(Fig. 1b)*, Parker Hannifin's Indego (*Fig. 2a)* and Cyberdyne's HAL (Hybrid Assistive Limb) *(Fig. 2b)* address medical applications. All have a similar architecture–an external frame attached to the operator using Velcro belts and shoes. With this configuration, the frame helps support the operator, and provides feedback to the system. The battery and control system are usually in a pack on the back of the upper part of the system.

Weight and strength are critical to designs. More weight complicates overall operation and increases power requirements, thereby reducing runtime. Lightweight composite materials help: Parker Hannifin's Indego, for instance, weighs in at only 26 lb.

Servos such as accelerometers are found in the joints and sensors, and are located throughout the systems. Feedback systems vary among devices. For example, Cyberdyne's HAL detects bio-electric signals (BES) generated by the brain to control muscles. Sensors are attached to the skin to detect BES so that the exoskeleton knows the particular desired movement.

The ReWalk Personal System was approved by the FDA in June 2014. Clinical trials are in progress for the other platforms. These system are often combined with arm crutches, giving a user additional support and movement control. This will depend on the user's requirements and capabilities.

Part of the design and deployment challenge is the size range of the operators. Weight and height are key factors for delivering multiple configurations or adjustable designs. Operating time varies, but is on the order of a few hours.

Ekso Bionics has a feature called Variable Assist, which allows clinicians to control the system's augmentation based on a patient's strengths and limitations. It allows weaker

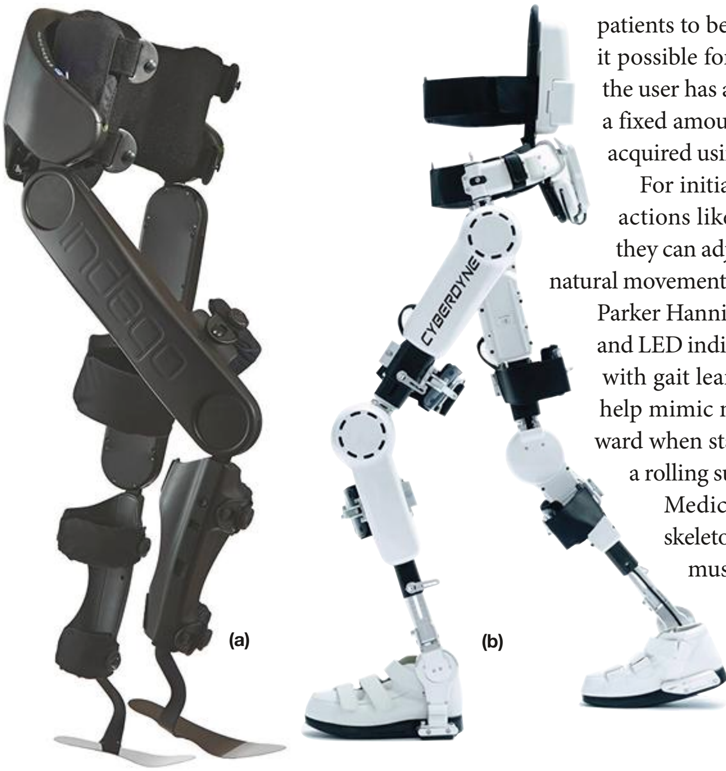

2. Indego's (a) and Cyberdyne's (b) offerings are good examples of state-of-the-art exoskeletons.

patients to become more stable quickly. The Adaptive Assist makes it possible for the system to dynamically adjust its support so that the user has a smooth and consistent gait. The Fixed Assist provides a fixed amount of power, and it is usually configured based on data acquired using the Adaptive Assist.

For initial training, Ekso's FirstStep allows clinicians to initiate actions like steps. ProStep support is used as patients progress; they can adjust their hips forward and move them laterally as more natural movement is achieved.

Parker Hannifin's Indego uses vibratory feedback to indicate balance and LED indicators to provide status, along with a mobile app to help with gait learning and teaching. The system uses postural cues to help mimic natural movement, including actions like leaning forward when standing up. The entire system breaks down to fit inside a rolling suitcase.

Medical use of exoskeletons is more demanding than exoskeletons that simply enhance movement. Not only must they must track the user's movements, but they also must provide correction or assistance to improve those movement. The exoskeletons also provide significantly more feedback to clinicians and doctors so that they can track a patient's progress.

EXOSKELETON RESEARCH

Exoskeleton research is pervasive, and firms like Hyundai Motor Company are pushing the envelope. The company is using tools like National Instruments' LabVIEW to design the control systems. The Hyundai Wearable Robotics for Walking

3. The HULC (Human Universal Load Carrier) uses hydraulics to provide heavy lifting capabilities.

Assistance system is controlled by a Single-Board RIO. The RIO architecture is based around an FPGA that proved valuable during the design process—the architecture changed several times, including drastic changes in the control architecture and sensor system. The new sbRIO-9651 System on Module (SOM) helped reduce the weight of the system by 10 kg while maximizing the battery efficiency.

The Hyundai design consists of two modules that can be used together or independently. These include the Hip Modular Exoskeleton and Knee Modular Exoskeleton.

The HULC (Human Universal Load Carrier) *(Fig. 3)* is a joint research project between Berkeley Robotics and Human Engineering Laboratory, Ekso Bionics, and Lockheed Martin for the U.S. Army Natick Soldier Research Development and Engineering Center (NSRDEC). It is designed to help soldiers carry up to 200 lb. of gear while reducing strain on the body. HULC needed to address rugged environments, including sand, wind, rain, and extreme temperature and humidity conditions.

> "Part of the design and deployment challenge is the size range of the operators. Weight and height are key factors for delivering multiple configurations."

The HULC's anthropomorphic design used hydraulics to provide lift. The on-board computer handles input from sensors and control of the hydraulic system. The system was designed in a modular fashion so that components could be easily replaced in the field. The system was also designed to support the full load even when battery power was low or exhausted.

TAKING THE LOAD

Providing mechanical assists to people can be done in a number of ways. For example, General Motors and NASA developed RoboGlove to help grip tools and objects *(see "Electromechanical Medical Marvels" on electronicdesign.com)*. This can help prevent problems such as cramps and repetitive stress, since the glove provides the compression instead of fingers.

Lockheed Martin's FORTIS *(Fig. 4)* is a mechanical engineer's dream. The unpowered exoskeleton is designed to offload the weight of heavy tools up to 36 lb. to reduce the stress on the operator. The U.S. Navy is interested in its potential to help with shipbuilding. The mechanical linkages

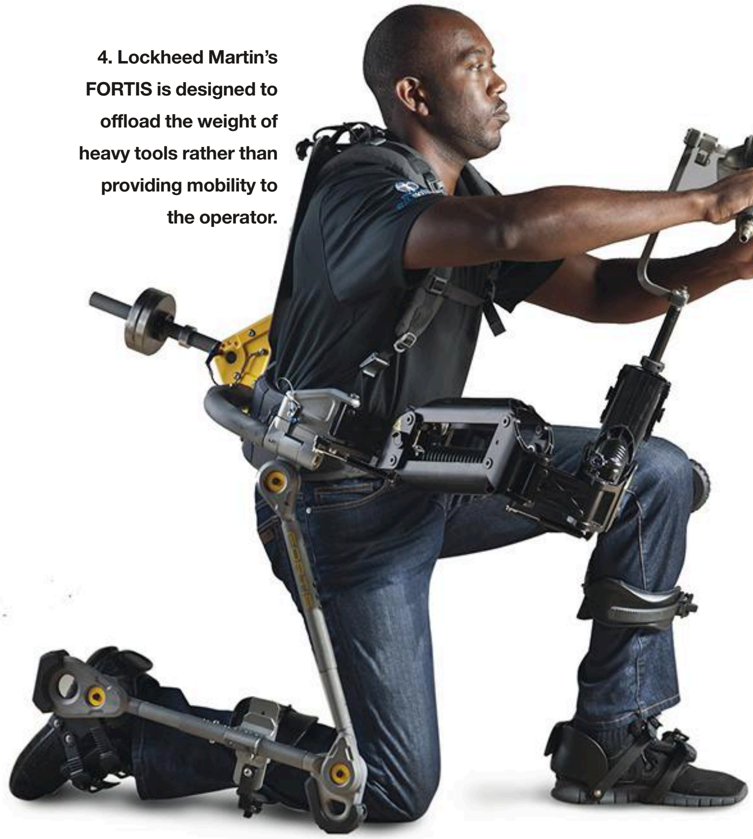

4. Lockheed Martin's FORTIS is designed to offload the weight of heavy tools rather than providing mobility to the operator.

transfer the load of the tools to the ground. The operator simply repositions the frame. Counterweights and support points allow tools to be used almost as if the operator was in a weightless environment. A zeroG Arm is attached to the thigh portion of the frame, and the tool is attached to a gimbal on the arm. The technology is very similar to that used in the Steadicams, which are often found on movie sets and filming of sporting events.

The advantage of FORTIS is that it reduces muscle fatigue by up to 300%, thereby increasing productivity. On top of that, the exoskeleton can help minimize the number of accidents that often take place while operating heavy equipment.

Exoskeleton development is continuing among these and other companies. In the future, look for reduced cost, increased capabilities, and a wider range of applications. Medical applications remain a primary focus for many involved in the system's design, but challenges still linger in terms of approval, availability, and cost. ed

Powerful, Versatile and Affordable...

100 kHz Dynamic Signal Analyzer

- ***DC to 100 kHz frequency range***
- ***100 kHz real-time bandwidth***
- ***Dynamic range***
  - ***90 dB (FFT)***
  - ***145 dB (swept-sine)***
- ***Low-distortion (–80 dBc) source***
- ***Up to 32 Mbyte memory***
- ***GPIB and RS-232 interfaces***

FFT analyzers starting at $4950

The SR785 Dynamic Signal Analyzer offers state-of-art performance at a fraction of the cost of competitive analyzers. Standard features include swept-sine mode, order tracking, octave analysis, curve fit/synthesis, and arbitrary waveform source.

When compared to the Agilent 35670A, the SR785 comes out on top. It offers twice the frequency range (2 ch.) and 10 times the real-time bandwidth at less than half the price of the 35670A.

The SR785 is ideal for filter design, control systems analysis, noise measurement, audio or acoustical test, and mechanical systems analysis.

Take a close look at the SR785.

SRS **Stanford Research Systems**
1290-D Reamwood Ave., Sunnyvale, CA 94089 • e-mail: info@thinkSRS.com
Phone (408) 744-9040 • Fax (408) 744-9049 • **www.thinkSRS.com**

UPAL SENGUPTA, DICK STACEY, and BILL JOHNS | Texas Instruments

Stay Up-to-Date with Wireless Power

New standards have emerged that allow for interoperability of charging surfaces and portable devices across different manufacturers, as well as higher efficiency and higher power levels up to several watts.

Combining wireless power with wireless connectivity makes it possible to design a completely sealed device with no external connectors. Consequently, wireless power is ideal for any portable equipment that needs to operate in outdoor or wet environments. Examples include wearable devices such as smartwatches or fitness bands, medical equipment (that must be washed or sterilized), or outdoor-use devices including cameras, communications equipment, or measurement instruments.

Wireless power has steadily gained popularity over the past several years. While it began as a means of improving end-user convenience in recharging mobile devices, it's now becoming a standard feature in several new applications. As the technology finds its way into a wider range of applications, specific solutions tailored to specific power levels will be required to optimize system-level performance. Magnetic component design, critical tuning capacitors, and, of course, the silicon components used for power conversion must all be properly selected to achieve the desired results.

TODAY'S LEADING STANDARDS

Three standards compete within the world of wireless power: the Wireless Power Consortium's WPC, the Power Matters Alliance's PMA, and the Alliance for Wireless Power's A4WP *(Table 1)*. All three employ the same basic physical principles to transmit energy. However, they use different combinations

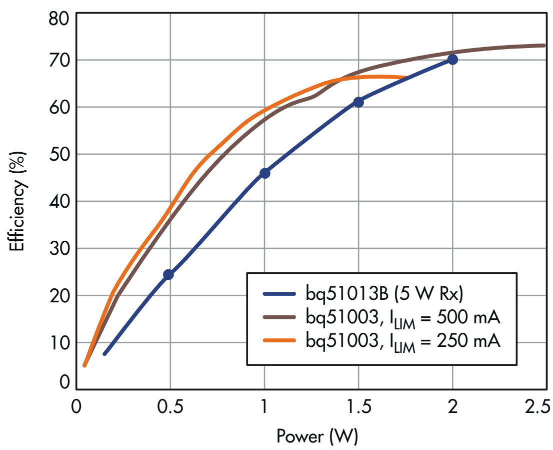

1. Here, efficiency is compared between 2.5- and 5-W receivers when operating at low-power levels. These curves use a TX coil measuring approximately 50 mm in diameter, and an RX coil of approximately 30 x 40 mm.

TABLE 1: TODAY'S COMPETING WIRELESS-POWER STANDARDS

	Wireless Power Consortium: WPC/Qi 1.1	Power Matters Alliance: PMA	Alliance for Wireless Power: A4WP
Coupling	Tightly coupled	Tightly coupled	Loosely coupled
Approximate frequency range	100 to 200 kHz	200 to 300 kHz	6.78 MHz
Communication path	In-band (signaling over the power path)	In-band (signaling over the power path)	Bluetooth Low Energy (BLE)/out-of-band (separate channels for power and control)
System-level efficiency	>70%	>70%	
Spatial freedom with existing standard	Medium	Lowest	Highest
Future planned enhancements	Qi 1.2 specification extension will add loosely coupled/ resonant capability to WPC standard	Merged with A4WP for future resonant implementation	

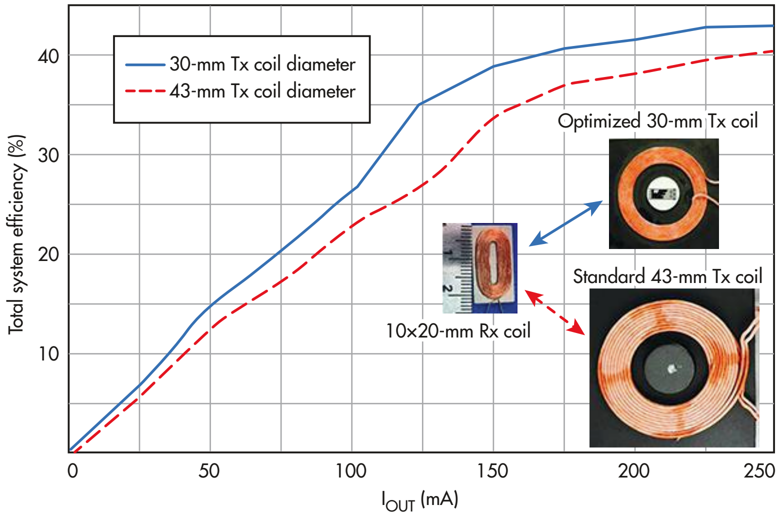

2. Efficiency can differ considerably between two different sizes of TX coils with a very small 10- x 20-mm oval RX coil. Total efficiency is lower than the example with a larger receiver coil at comparable power levels. However, it can be improved by reducing the TX coil size closer to that of the small RX coil.

of frequency, coupling constant (K) and inductor Q factors.

WPC and PMA use high-K (lower positional freedom) and can operate with lower-Q inductors. Both WPC and PMA are relatively low-frequency compared to A4WP, which means they have higher inductance values (i.e., in the range of several microhenries).

Tightly coupled, near-field systems also have relatively high efficiency. However, they require precise placement and alignment of the receiver (battery-powered device) to the transmitter (charging pad).

A4WP is designed to operate as a loosely coupled system, so the coils needn't be precisely aligned. The notable advantage of this system is its high positional freedom. Thanks to that freedom, the receiver (portable device) can be placed in a wider area relative to the charging surface. This provides extra convenience to the end user. Its higher frequency (6.78 MHz) allows for the design of high-Q/low-inductance values for the RX coils.

This system is technically more complex than the lower-frequency, closely coupled systems. It could very well grow in popularity, though, as technical challenges become resolved in the future.

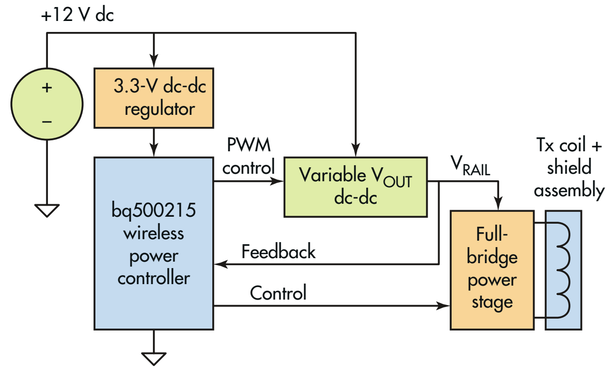

3. When the RX in a typical 10-W system requires more output power, it requests that the transmitter increases the voltage on the dc rail. When the RX load decreases, V_{RAIL} also decreases.

OPTIMIZED SOLUTIONS FOR 2-, 5-, 10-W APPS

The first WPC/Qi standard, which led to broad adoption of wireless power in smartphone applications, was targeted to meet 5-W output-power capability. This power level corresponds to the typical one- to two-hour charging time common for smartphone applications (roughly 1-A charge rate into a single-cell Li-ion battery). However, as applications for wireless power become more diversified, power circuits can be optimized to match different needs.

(continued on p. 24)

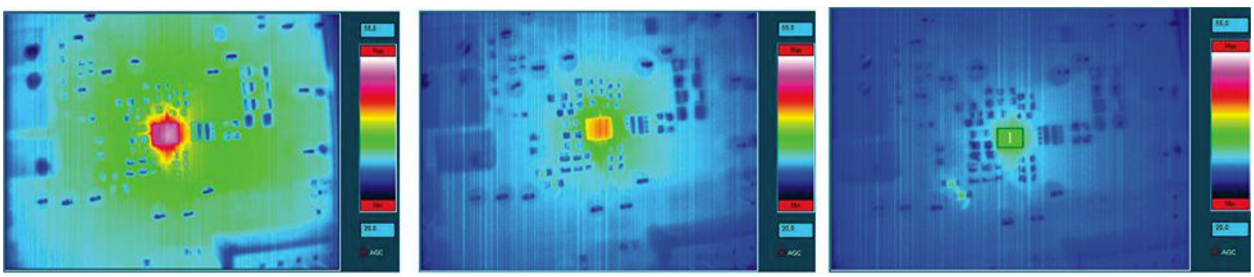

4. The 10-W receiver can be operated at 5-, 7-, or 10-V output settings. The 10-V setting results in the least amount of heat generated. Thus, it should be used if a high-efficiency switch-mode converter (e.g., the bq2419x series) is available for battery charging.

Smartphone devices typically use batteries in the 1500- to 3000-mAH range, while batteries for common wearable devices might range from 50 to 300 mAH. Thus, wearable-device battery-charge rates (and physical sizes) are correspondingly smaller. Though wireless-power transfer efficiency is generally lower at these power levels, thermal management still can be a concern due to the small size and limited area available for heat dispersion. Conversely, newer smartphones and tablets are increasing their battery size to accommodate larger displays and higher processing-power demands.

Other applications, such as industrial handheld terminals, also may require larger batteries and higher battery voltages (e.g., two-series Li-ion packs), which need more output power.

Production-ready solutions are now available and optimized for less-than-2-W, 5-W, and 10-W power-class devices. *Table 2* summarizes the appropriate combination of TX and RX controllers, and magnetic component sizes.

SPECIAL CONSIDERATIONS FOR LOW-POWER/WEARABLE APPS

For a low-power application, total system efficiency is enhanced by using the right wireless power receiver. One example is TI's bq51003, which is optimized for efficiency at low power *(Fig. 1)*.

In low-power applications, small size is often a key consideration for devices such as remote sensors or wearable products. Typical 5-W, inductively coupled, wireless-power systems have TX coils in the 40- to 50-mm diameter range; RX coils fall in the same general size range (35 mm across or larger). But if the RX coil shrinks below 25 mm in diameter (typical for small wearable products), its efficiency will degrade significantly when paired with a standard TX coil, and in some cases may not start up reliably. In general, if the TX and RX coil sizes are comparable, the coupling factor (K) is optimized *(Fig. 2)*.

> "Three standards compete in the world of wireless power: the Wireless Power Consortium's WPC, the Power Matters Alliance's PMA, and the Alliance for Wireless Power's A4WP."

OPTIMIZING FOR HIGHER POWER

To extend power capability to 10 W, several additional points must be considered. First, the silicon power components must be designed to handle the peak and continuous power levels. On the transmitter side, power-FET components are external to the transmit controller, so they can be scaled up as needed to handle peak currents. On the receiver side, where a physically small solution is important, integrated FET devices are used to provide a single-chip implementation. The FETs in the RX controller must provide lower R_{DS_ON} (relative to the 5-W receivers) to enhance efficiency and thermal performance.

TABLE 2: TX/RX COMBINATIONS FOR DIFFERENT POWER LEVELS

Power level	TX device	Typical TX coil size	TX input voltage	RX device	Typical RX coil size	RX output voltage	Companion battery charger
<2 W	bq500212A	30-mm round	5 V	bq51003	20-mm round or smaller	5-V fixed	bq25100
3- to 5-W smallest size	bq500212A	50-mm round	5 V	bq5105x (direct charging)	30- x 40-mm rectangular	4.2- or 5.35-V regulated charger options	Not required
				bq51013B (regulated dc output)		5-V fixed	bq2407x (linear); bq2425x (switch mode)
5-W highest efficiency	bq500212A	50-mm round	5 V	bq51021	40- x 40-mm rectangular	5- to 8-V adjustable	bq2425x
5 W with wider RX placement area	bq500412	Three overlapping coils; total approximately 55 x 100 mm	12 V	bq51021	40- x 40-mm rectangular	5- to 8-V adjustable	bq24250
10 W	bq500215	50-mm round	12 V	bq51025	40- x 40-mm rectangular	5- to 10-V adjustable	bq2419x (1-cell applications); bq2417x (2-cell applications)

Magnetic components (TX and RX coils) must also be rated to handle higher peak currents needed for 10-W power transmission. Finally, because the magnetic field strength will be higher for a 10-W system, the receiver-side shielding must be larger (compared to a 5-W system). This will provide better shielding for the system's metal components, as well as minimize "friendly metal" losses on the receiver side.

Recall that in *Figure 1*, the RX controller provides feedback to the TX controller, asking the TX to vary its output power

(continued on p. 38)

WILLIAM WONG | Technical Editor

Type-C Connectors
Seize Multi-Interface Versatility

The USB 3.1 Type-C connector has dominated the USB space, but now it's branching out toward other platforms such as DisplayPort.

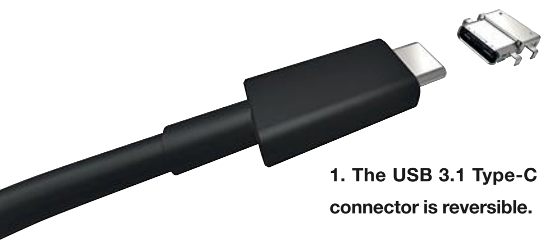

1. The USB 3.1 Type-C connector is reversible.

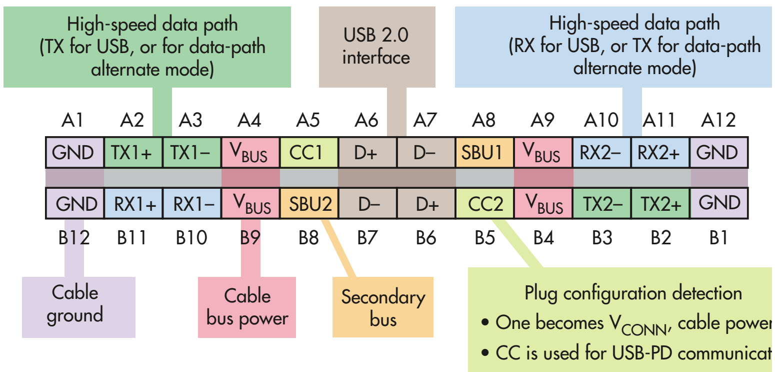

2. The 24-pin USB 3.1 connector has multiple interfaces, including a configuration bus.

s the VESA USB 3.1 Type-C connector *(Fig. 1)* the one connector that will rule them all? It may very well be the only connector on host devices like smartphones, tablets, and laptops in the future, with its ability to handle a range of interfaces beyond USB 3.1. It's also reversible and can carry more power. Of course, with signals running at 10 Gb/s, the USB connection can be a challenge to test.

So, what's behind this multilingual, "alternate mode" nature of the Type-C connection? To start with, the 24-pin connector *(Fig. 2)* has multiple communication links, including a USB 2.0 and high-speed serial interface that defaults to USB 3 (it runs independently of the USB 2.0 interface on different pins). Also, a configuration interface controls power and the high-speed path, which provides the multiprotocol support.

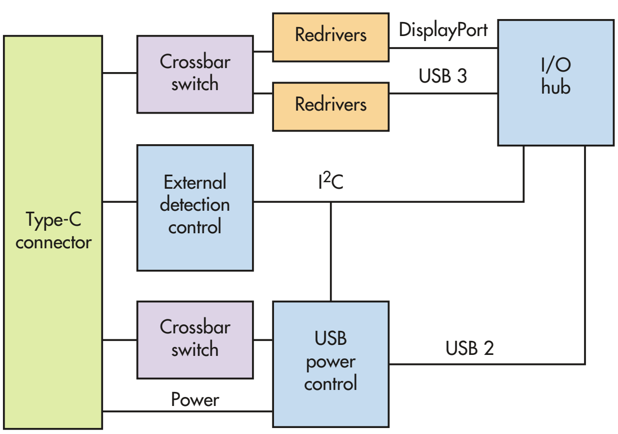

3. A dual protocol interface uses a crossbar switch controlled by the External detection control unit to switch between USB 3.1 and another interface (e.g., DisplayPort).

Essentially, the two devices at either end of the cable negotiate the interface to be used with the high-speed serial connections *(Fig. 3)*. A crossbar switch redirects the Type-C connections to the appropriate redrivers connected to the host's I/O hub. The External detection control tackles overall configuration (including determination of the host device, where appropriate) as well as USB power management. A USB 2.x device was limited to 500 mA or 2.5 W, while USB 3.1 handles up to 100 W.

For now, multichip solutions are the most likely to implement connections supporting more than one interface. In the future, though, look for popular platforms to emerge with combinations like USB 3/DisplayPort. These will often be found on host devices (e.g. smartphones, tablets), but alternate-mode operation makes sense in other scenarios. For example, a display device might support DisplayPort, USB 3, and even PCIe, and thus could be driven by a host with only one of these interfaces.

These small Type-C connections come in various forms to address a range of installations. The key is that the same connector is at both ends of the cable, compared to the typical USB cable with a different connector at each end. ed

ANATOLIY TSYRGANOVICH, LEONID NEYMAN, and ABDUS SATTAR
IXYS Corp.

Limit Inrush Current in AC-DC POWER SUPPLIES and RECTIFIERS

An innovative inrush-current device takes advantage of a unique control algorithm to mitigate issues surrounding the large currents often needed to charge up bulk capacitors.

Rectifiers and ac-dc power supplies employ large bulk capacitors. During power-up, these capacitors require a large amount of current to charge up, resulting in a large inrush current. This inrush current creates limitations in the operation of power devices and interference of those devices with the power line and circuit breakers. It also affects the reliability of the power system due to overstress caused by instantaneous but huge surge in initial current at power up. Known solutions to limit inrush current[1,2] require resistors or conventional NTC thermistors, which contribute significantly to power loss and subsequently decrease the efficiency.

To overcome many of the existing technology's disadvantages in limiting inrush current in high-power ac-dc power supplies and rectifiers, IXYS developed the Digital Inrush Current Controller. It combines the company's digital power-control technology with Zilog's 8-bit Z8F3281 MCU to limit capacitor pre-charge current to a predetermined value at each half sine-wave cycle. Capacitor charge is spread over a number of cycles until the capacitor is charged proportionally to a peak value of ac voltage source.

The controller features programmable overload protection and a "Power Good" status signal. It's not sensitive to power outage, brownout, and ambient temperature variations. It can operate over an input-voltage range of 80 to 240 V ac, and load current up to 3 A. The entire operation's process and essential values are fully programmable—the controller may be programmed to 50 Hz, 60 Hz, or any other line input frequency operation.

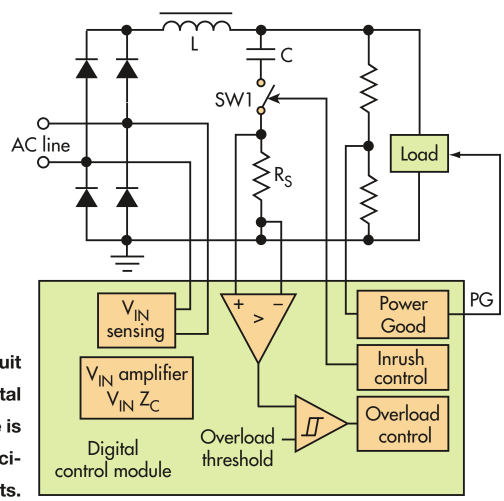

1. In this conceptual circuit schematic for a digital inrush controller, charge is delivered to the bulk capacitor in equal increments.

TIME-DEPENDENT PULSE TRAIN

Figure 1 illustrates a conceptual circuit schematic that's designed to deliver charge to the bulk capacitor in equal increments. The capacitor is charged according to a time-dependent pulse train driving transistor SW1. The pulses are designed in a way to provide substantially equal voltage increments to the capacitor to keep peak charging current at about the same value for each cycle. The number of cycles depends on the capacitor value, and selection of the charge current correlates to the desired ripple's amplitude at the output. Charge current is a function of the number of pulses and the timing position with respect to the rectified sine wave.

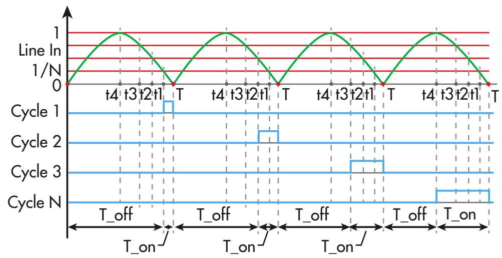

2. This example of digital inrush control timing generates a pulse train for transistor SW1.

Figure 2 shows an example of generating the pulse train for SW1. If we can consider N cycles for inrush control, then we can split the normalized amplitude of half-rectified sine wave to N segments with an increment of 1/N as shown. During cycle 1, SW1 is on (conducting) from the time stamp *t1* to *T*, thus making the capacitor C charge to the voltage proportional to normalized value 1/N. The charging current doesn't rise instantly because it's a current in a serial LC resonant circuit that shapes the current waveform to the resonant one. The current rises until the capacitor's voltage reaches input voltage.

Subsequently, current continues its resonant behavior because SW1 is still conducting. No further oscillation occurs because input voltage drops below voltage on the capacitor, and then SW1 is off (not conducting). The

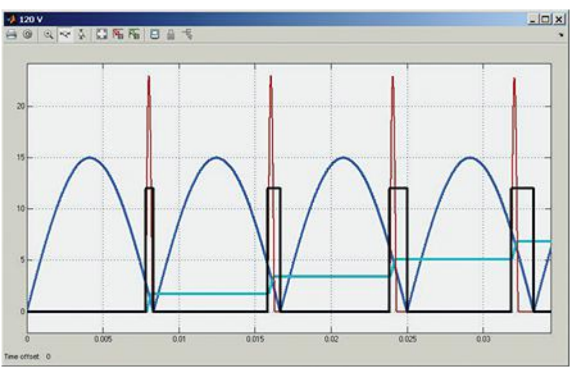

3. To illustrate *T_on* timing generation, a conceptual algorithm was executed in the MCU Z8F3281 for the first four cycles of inrush control. Here, blue = rectified power-line voltage; red = power-line current; black = on-time *T_on* for SW1; and green = capacitor's voltage (not to scale).

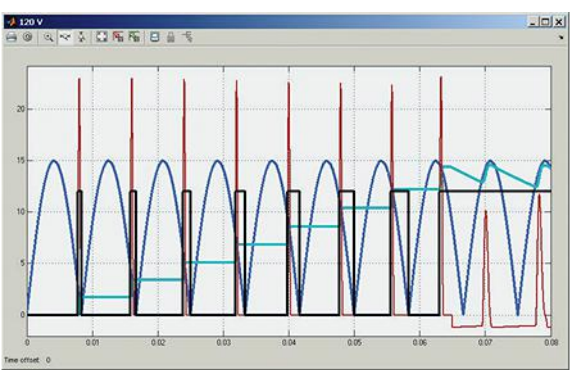

4. Results for the precharging of the capacitor shows the timing position and amplitude of capacitor's current (red curve) with respect to *T_on* pulses. Here, blue = rectified power-line voltage; red = power-line current; black = on-time *T_on* for SW1; and green = capacitor's voltage (not to scale).

capacitor remains pre-charged to the voltage proportional to 1/N. In Cycle 2, capacitor C is pre-charged by another voltage increment 1/N in the process similar to cycle 1. Capacitor C is charged N cycles to the voltage value proportional to the input-line voltage.

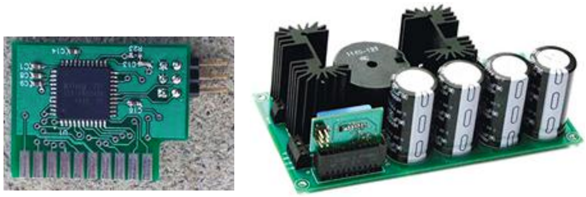

5. IXYS's Digital Inrush Controller incorporates an MCU module (a) and a main power board, shown here with MCU module (b).

PRINCIPLE OF OPERATION

Another variable to control inrush current is LC time constant. Capacitor C value depends on desired ripple value. After selecting the capacitor C value, the designer can decrease peak inrush current by increasing inductance L. If there are physical limits to the L value, the number of cycles N should be used to set the required peak current. Turn-on time for switch SW1 should be defined for each active cycle.

For cycle 1 in *Fig. 2*, the delay from the zero crossing point *(point 0 in Fig. 2)* to the beginning of turning on SW1 *(t1)* is denoted as *T_off*. The time between *t1* and *T*, an active time to keep SW1 on, is denoted as *T_on*, and the period or cycle duration is denoted as *T*.

Active time *T_on* for each occurrence "i" is defined as geometrical transform:

$$T_{on(i)} = \frac{T}{\pi/2} \text{a sin}(i/N) \qquad (1)$$

where i = 1… N.

The period T is measured by the MCU at initialization. Values of *T_on* are determined by Equation 1 and stored in memory. Values of *T_off* are derived by firmware according to the following expression:

$$T\_off = T - T\_on \qquad (2)$$

Figure 3 illustrates a conceptual algorithm that's executed in MCU Z8F3281 for the first four cycles of inrush control. The timing counter corresponds to time at any given moment of a discrete time base provided by the internal clock. The counter first counts from zero crossing to the *T_off* value. When the counter reaches the *T_off* value, it initiates a *T_on* pulse *(black line on Fig. 3)* that continues until the counter reaches the *T_on* value, finalizing one charging cycle. The rectified power-line voltage (blue line) is shown for reference.

Figure 4 illustrates the timing position and amplitude of the capacitor's current *(red curve)* with respect to *T_on* pulses. It should be noted that the Inrush Controller generates a single current pulse during each cycle. The capacitor's charge is complete when input voltage drops below capacitor voltage. The input power line is isolated from the rest of the circuitry by the diode bridge circuit, and the inductor discharges into the capacitor. Then SW1 is turned off (not conducting) up to the end of the cycle. The algorithm is based on reactive power transfer, hence, losses are limited mostly to those on strain resistance.

Figure 4 shows that the capacitor's precharge is finalized at time-stamp 0.066 ms. After that, the Power Good (PG) signal is generated and load is activated. The capacitor's current shows up as negative beginning at time-stamp 0.066 ms, because current is sourced from the capacitor when the load is activated. The PG signal can be delayed with respect to end of pre-charge of capacitor C so that the load can stabilize before executing other functions. The overload threshold is programmable, too, and is set to 3.5 A.

OVERLOAD PROTECTION

Overload protection protects a device from damage in case of overload or continuous overload. If a comparator

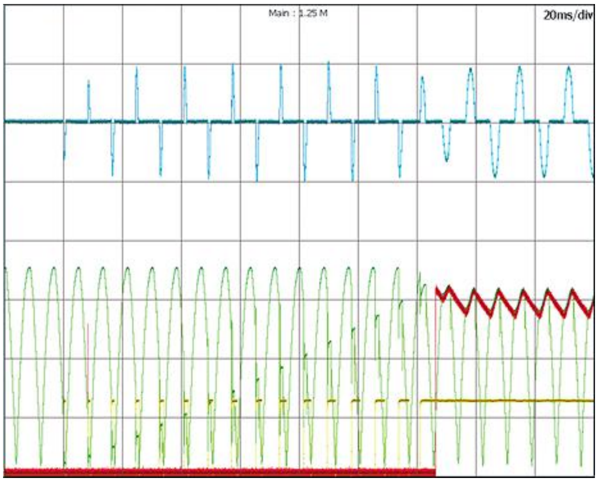

6. Several bench tests helped verify the Controller's performance, such as this scope snapshot of the digital inrush current control. Here, blue = power-line current (10A/div); red = load voltage (50 V/div); green = rectified input voltage (50V/div); and yellow = SW1 drive signal.

detects overload, then the MCU disconnects the capacitor from the load by turning off SW1. Also, the PG signal is set to logic low to disable the load if possible. Overload protection can be programmed for two modes of operation: immediately shut down the device and wait for user interference; or allow a device to restart a predetermined number of times.

After initial pre-charging and connecting the load, the MCU may be reconfigured for other power-management tasks. For example, it can perform power-factor-correction (PFC) control and keep track records on device performance, overload conditions, power outages, power brownouts, etc. With the collected information, the MCU is able to inform the user on the state of the device's reliability and supply system performance data.

DIGITAL INRUSH CONTROLLER

IXYS's Digital Inrush Controller consists of an MCU module and main power board *(Fig. 5; for detailed schematics of these two parts, see the online version of this article at www.electronicdesign.com)*. The MCU module, implemented as an add-on device, has a connector for MCU programming. The MCU should be programmed before powering the entire system. An auxiliary power supply powers the module, providing +3.3 V for the MCU and 12 V for the gate driver applied to connector J4 on the main power board.

The main power board is a two-layer printed-circuit board (PCB) with a diode bridge and MOSFET Q1 (SW1) mounted on small heat sinks. Power dissipated on these heat sinks is less than 5 W at 375-W output power. This board may be powered from a 50- or 60-Hz ac source.

INRUSH-CONTROLLER TESTING

The controller's performance has been verified by several bench tests, such as that revealed in the scope snapshot in *Fig. 6*. Testing confirmed that the inrush current is limited to a predefined value and limiter performance is quite close to simulation results. The amplitude of the inrush current is limited to the value of the input current at maximum load by selecting the number of inrush current pulses equaling 16 and the inductor value to 100 µH. It minimizes the negative impact on the ac line, and limits electromagnetic interference (EMI).

During the test, the ac input line is connected through an isolation transformer as a precaution. The Power Good signal's connecting load is generated at the rectified voltage zero crossing one cycle after the output capacitor is completely charged *(see the red line in Fig. 6)*.

(continued on p. 37)

Bicolor LED Indicates Voltage Readings Via Visual Pulses

RICARDO JIMÉNEZ and KIMBERLY D. VARELA | Instituto Tecnológico de Mexicali (ITM)

THE CIRCUIT IN *Figure 1* uses a bicolor (red/green) LED to indicate the voltage measured with a set of three color pulses. The green, yellow, and red pulses indicate the units, decimal point, and decimals of volt, respectively.

The circuit is based on the 8-pin MCU PIC 12F683. It requires only two I/O lines to display a voltage reading with a resolution of 0.1 V. The period of the LED pulses can be adjusted from 1 to 255 ms with the trimming potentiometer (trimpot) connected on AN3. With this trimmer, users can set the refresh rate to suit their needs. The software program occupies only 280 words out of the 2 kB of available program memory.

The input voltage range measured on pin AN0 ranges from 0 to 5.00 V dc and the total current consumption is 5 mA, with precision of ±19.6 mV. A trimpot connected to that analog input is used to read an input voltage, and the second trim pot connected to AN3 adjusts the period of the pulses to users' needs. To save energy, the analog-to-digital converter is turned off between each reading.

Figure 2 shows a set of train pulses in the scope for a voltage reading of 2.4 V. Notice that the two pulses on the top line represent two volts (green LED), then a single pulse in the middle indicates the decimal point (yellow color), and the bottom line has five pulses (red LED). *Figure 3* shows the physical circuit assembled on a prototyping board.

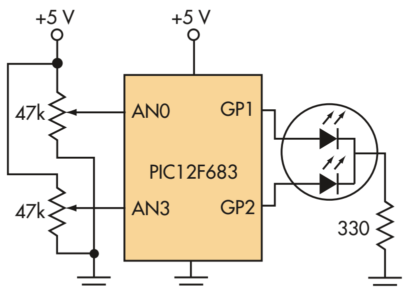

1. This fairly simple circuit uses a standard bicolor LED and an MCU, plus three resistors, to indicate a voltage reading, with both reading measurement and LED readout managed by a short coded algorithm; neither layout nor components are critical.

The algorithm provided in the flowchart *(Fig. 4)* is based on PIC Basic Pro Compiler (see the listing). It starts by measuring the input voltage to detect its range with five magnitude comparisons for the volt's units. There are five different ranges for the full scale of five volts. If the voltage is less than 1 V, for example, the yellow LED will pulse the decimal point, then the red LED will display the decimal value of the voltage with the corresponding number of pulses. Once the unit's voltage range is detected, the program makes 10 comparisons to find the range in 100-mV increments. In this way, it will generate the correct number of pulses for the decimal value of volts.

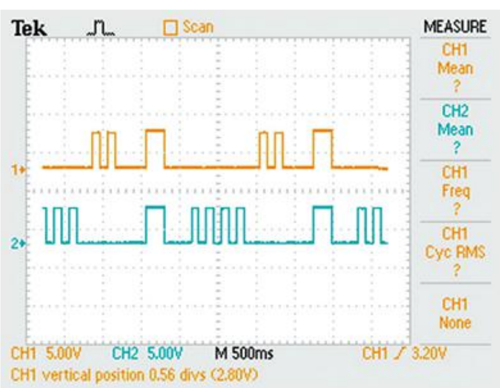

2. In these digital pulses for a measurement of 2.4 V dc, the orange pulses represent units of volt. Then both lines go high to indicate the decimal point, and finally the four blue pulses represent 0.4 V dc.

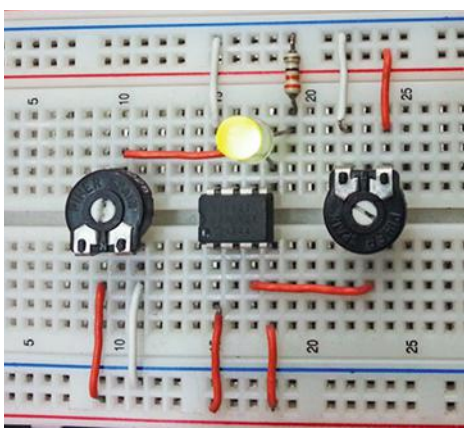

3. A protoboard assembly for the PIC 12F683 required only a bicolor LED to indicate a voltage input using a set of three different color pulses.

DESIGN NOTES

Dual 9A, Step-Down μModule Regulator with Digital Power System Management

Design Note 542

Jian Li, Yingyi Yan and Marvin Macairan

Introduction

The LTM4675 is a dual 9A or single 18A step-down μModule® (micromodule) DC/DC regulator featuring remote configurability and telemetry monitoring of power system management (PSM) parameters over PMBus—an open standard I^2C-based digital interface protocol. Its 16mm × 11.9mm × 3.51mm BGA package includes analog control loops, precision mixed-signal circuitry, EEPROM, power MOSFETs, inductors and supporting components. It features a wide 4.5V to 17V input voltage range, and a 0.5V to 5.5V output voltage range with ±0.5% DC accuracy over temperature. LTM4675's power outputs can be digitally adjusted, margined and powered up/down at programmable slew rates and sequencing delay times. Maximum turn-on time is 70ms. Telemetry read back parameters include V_{IN}, I_{IN}, V_{OUT}, I_{OUT}, temperature, running peak values, uptime, faults and warnings. Current read back accuracy is ±2.5% at 9A load over temperature.

The LTM4675 facilitates the design of high efficiency, high power density and high reliability solutions for telecom, datacom and storage systems, plus industrial and instrumentation power supplies. The LTM4675 is offered in a 16mm × 11.9mm × 3.51mm BGA package available with SnPb or RoHS compliant terminal finish.

Dual 9A μModule Regulator with Digital Power System Management

Figure 1 shows a typical LTM4675 application. The input voltage range is 5.75V to 17V, and the outputs are 1V/9A and 1.8V/9A. Figure 2 shows the efficiency

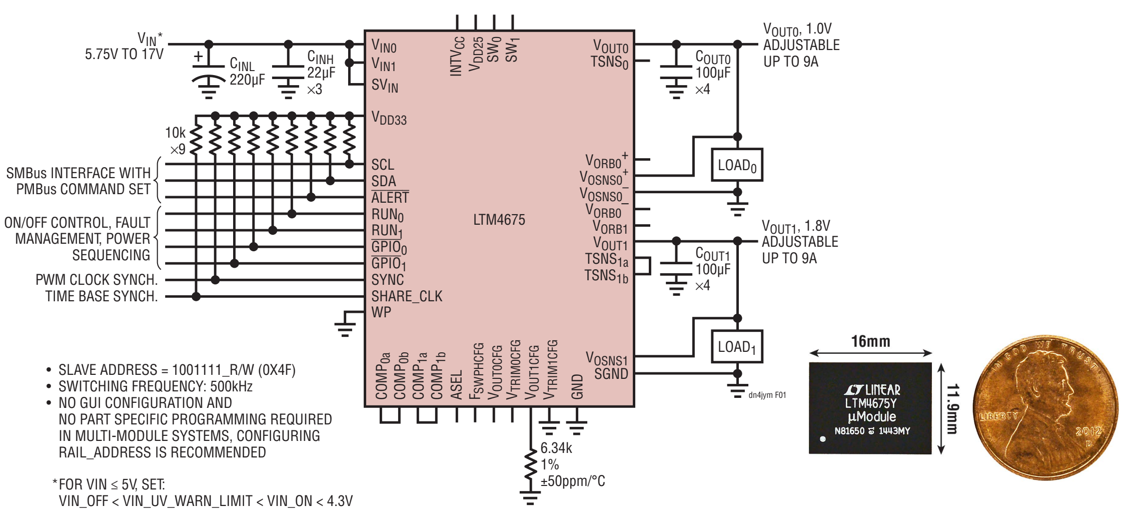

Figure 1. 9A, 1V and 9A, 1.8V Output DC/DC μModule Regulator with Serial Interface

for each output of the LTM4675 for a variety of output voltages vs load current. The LTM4675 can achieve high efficiency over a wide operating range, with high reliability. Figure 3 shows that the maximum case temperature is 84.1°C when the module is running with a 12V input, 1V/9A and 1.8V/9A outputs, without airflow.

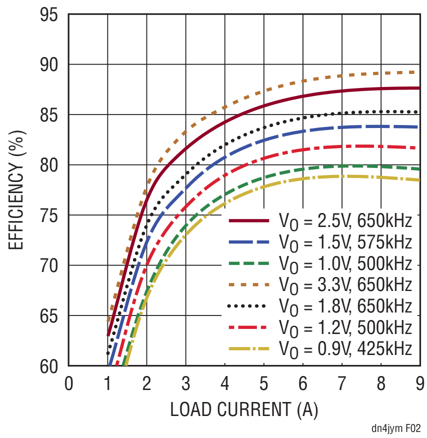

Figure 2. LTM4675 Single Channel Efficiency at V_{IN} = 12V

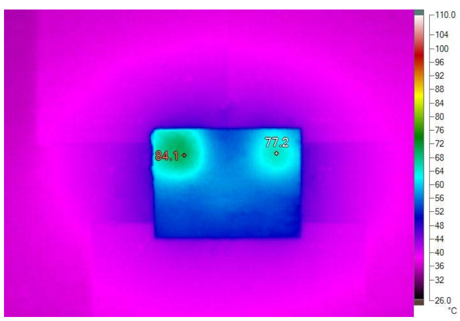

Figure 3. Thermal Performance of LTM4675 at V_{IN} = 12V, V_{OUT0} = 1V/9A, V_{OUT1} = 1.8V/9A, No Airflow, Tested on DC2053A. Maximum Temperature Rise = 61.1°C, T_A = 23°C

The LTM4675 offers internal compensation or external compensation, which can be used to optimize the transient response to load current steps over a wide operating range.

The LTM4675 supports a PMBus-compliant SMBus serial interface up to 400kHz. Readable data includes input and output voltages, currents, temperatures, running peak values, uptime, faults, warnings and an onboard EEPROM fault log record. Writable data and configurable parameters include output voltage, voltage sequencing and margining, digital soft-start/stop ramp, OV/UV/OT, UVLO, frequency and phasing. The LTM4675 guarantees high accuracy telemetry read back with an integrated 16-bit ΔΣ ADC.

Multi-Module Operation for High Current Applications

The LTM4675 utilizes a constant frequency peak current mode control architecture, which enables cycle-by-cycle current limit and easy current sharing among phases when the channels are operated in parallel. For higher output current capability, it's easy to parallel multiple LTM4675 modules. Furthermore, the LTM4675 can be used as a master to drive non-PSM power modules to provide much higher output current. For example, the LTM4675 can drive three LTM4630s to provide up to 125A output current. Figure 4 shows the thermal picture of this application. With 400LFM of airflow, the hot spot temperature rise is only 66.2°C. The uniform thermal distribution among the modules is due to excellent current sharing performance.

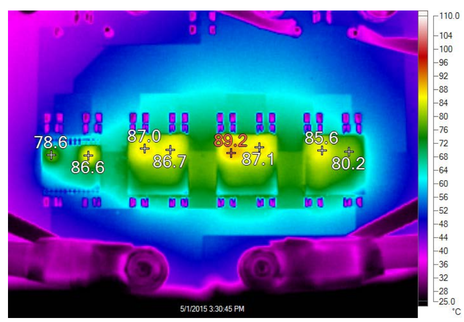

Figure 4. Thermal Picture at V_{IN} = 12V, V_O = 1.0V/125A, 400LFM Airflow, Maximum Temperature Rise = 66.2°C, T_A = 23°C

Conclusion

LTM4675 is a high efficiency and high power density µModule regulator with built-in digital power system management. With all of the features mentioned above, the LTM4675 is ideal for telecom, datacom and storage systems, industrial and instrumentation applications.

Data Sheet Download

www.linear.com/LTM4675

For applications help,
call (408) 432-1900

Linear Technology Corporation
1630 McCarthy Blvd., Milpitas, CA 95035-7417
(408) 432-1900 • FAX: (408) 434-0507 • www.linear.com

dn542f LT/AP 0915 111K REV A • PRINTED IN THE USA

The energy efficiency and compact size of this design suit it for diverse applications. It can be used to represent other variables using the PWM code in the microcontroller. In this case, the PWM can drive an LED in multiple ways by controlling its duty cycle and, therefore, the power dissipated. In addition, it can transmit a reading with a pair of LEDs (transmitter/detector) to monitor an input voltage at a limited distance.

RICARDO JIMÉNEZ holds a master's degree in electronics from ITM. He is an adjunct professor at Imperial Valley College, Imperial, Calif., and at ITT-Tech in Vista, Calif. He can be reached at ricardo.jimenez@imperial.edu.

KIMBERLY D. VARELA holds an electronics engineering degree from ITM.

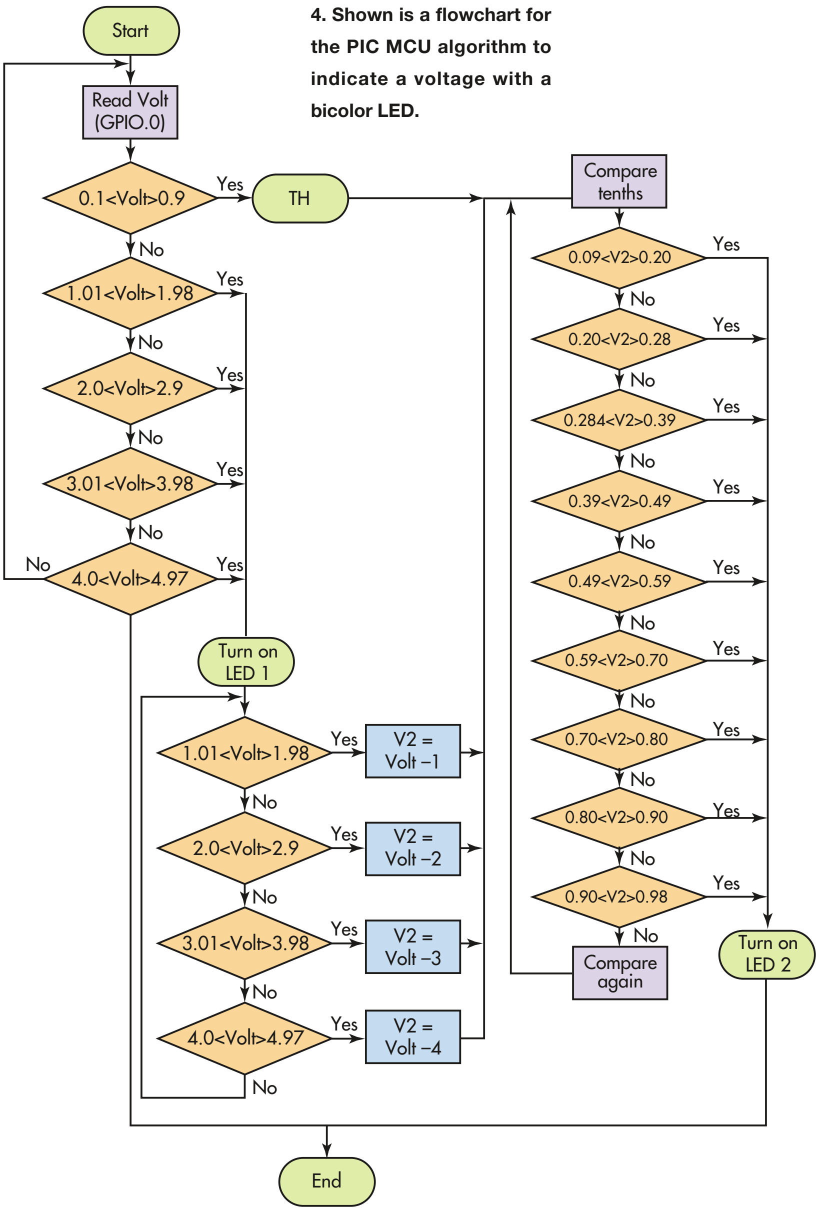

4. Shown is a flowchart for the PIC MCU algorithm to indicate a voltage with a bicolor LED.

CONFIDENCE LEVEL: HIGH

Microcontroller Generates Analog Gaussian Waveform Without Need For A DAC

DEV GUALTIERI | TIKALON LLC gualtieri@ieee.org

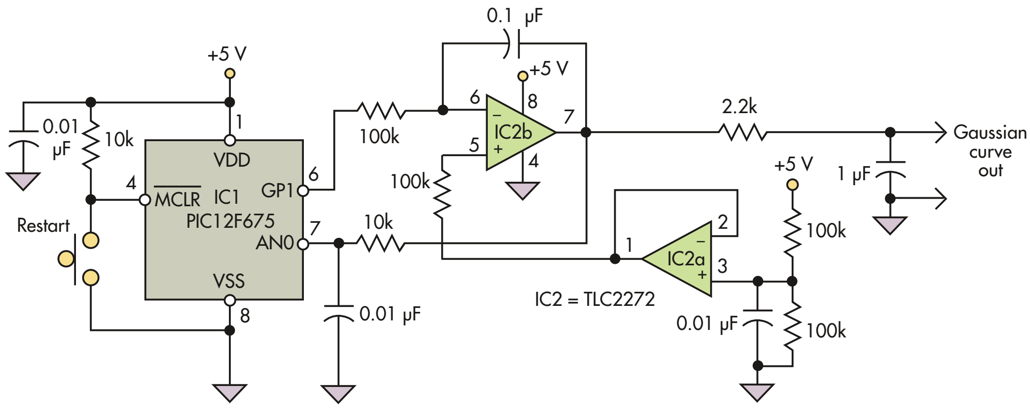

1. The Gaussian curve generator circuit takes advantage of the dynamic reassignment functionality of a microcontroller's I/O pin, operating in coordination with an op amp functioning as an integrator.

LABORATORY DATA OFTEN appears as Gaussian curves. Today's laboratory data-acquisition software is designed to analyze these data to determine peak location, amplitude, area, width, and more. A good test signal is useful in developing such software, and it is best when the test signal resembles actual analog data including noise.

Many years ago, while I was still a student, a professor and I built a few Gaussian-curve generators for students to use in a teaching laboratory. Since those were the days before inexpensive microcontrollers, you can imagine the complexity of such circuitry.

Fast forward a few decades, and I needed a Gaussian-curve generator for a software-development project. Of course, it's always possible to generate an arbitrary waveform with a microcontroller and a digital-to-analog converter (DAC). Although inexpensive microcontrollers include high-resolution analog-to-digital converters (ADCs), DACs are peripheral components.

The simple microcontroller circuit generates an analog Gaussian curve without needing a DAC *(Fig. 1)*. The key to the design is that most microcontrollers allow their I/O pins to be dynamically reconfigured to function as either a high-impedance input or as an output. The analog core of the circuit is an operational-amplifier integrator (IC2b) whose reference voltage is set at half the supply voltage by the other half (IC2a) of a dual package.

When microcontroller output (GP1) is in its high-impedance state, integrator IC2b neither charges nor discharges, so the output voltage is constant. When the output voltage as read by the microcontroller's analog input (AN0) shows that more output voltage is required, the software sets GP1 to its low-voltage state, so the integrator will charge.

When too high a voltage is sensed, GP1 is set to its high-voltage state, and the integrator will discharge. The software shown in the pseudocode listing is designed so this servo loop is damped to prevent excessive "seeking" around the setpoint voltage, as the output shows *(Fig. 2)*. The voltage values for the Gaussian curve, or another desired waveform, are generated by a timer interrupt routine that accesses a lookup table. The actual source code is available from the author by request.

Rail-to-rail op amps like the one used in this circuit don't function well with signals near the rails, so getting a true zero-voltage signal isn't possible with a unipolar supply. Bench measurements on the circuit show a minimum voltage of about 30 mV when driving a high-impedance load. Also, this approach to voltage generation won't work for rapidly changing signals. For the 4-MHz processor used, two updates per second are about the limit.

The internal memory of the PIC 12F675 microprocessor is limited to just 128 8-bit bytes, which allows for just a small lookup table. By using a linear interpolation of adjacent data points, you can double the temporal resolution. Since the curve is symmetric, the temporal resolution can be doubled again.

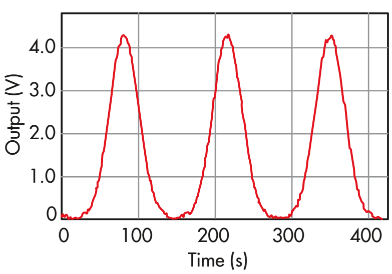

2. The noise, as seen in this "strip chart" trace of the circuit, mimics a typical data signal.

```
main()
{
//set I/O pin states, ADC, etc.
initialize_microcontroller();

output_pin = high-Z_digital_input;

/* set voltage generally obtained through a
timer interrupt routine and table look-up */

v_set = 500;

while(1) //Infinite loop
{
v = analog_voltage(analog_pin);
if (v>v_set)
{
delta = v-v_set;
output_pin = 1; //discharge integrator
//discharge for a time proportional to error
pause(delta);
output_pin = high-Z_digital_input;
}
else
{
if (v_set>v)
{
delta = v_set-v;
output_pin = 0; //charge integrator
//charge for a time proportional to error
pause(delta);
output_pin = high-Z_digital_input;
}
}
//continue infinite loop
}
}
```


DEV GUALTIERI received his PhD in solid-state science from Syracuse University in 1974. After many years in research for a major aerospace company, he now does computer, electronic, and embedded systems projects at his consulting company, Tikalon LLC, Ledgewood, N.J. He is the author of several books and can be reached at gualtieri@ieee.org.

IDEAS FOR DESIGN WANTED

Send us your Ideas For Design. We'll pay you $150 for every Idea For Design that we publish. In addition, this year's top design as selected by our readers will earn an additional $500, with two runners-up each receiving $250. You can submit your Ideas For Design via:

- E-mail: roger.engelke@penton.com

OR BY

Postal mail to:

Ideas For Design
Electronic Design
1166 Avenue of the Americas, 10th Floor
New York, NY 10036

Go to *www.electronicdesign.com* for our submission guidelines.

SMA RF Connector Designed for Microwave and Low Frequency

INTELLICONNECT'S new SMA Male connectors for 0.141 and 0.085 mm diameter cables are designed for use in microwave as well as low-frequency applications where size, performance, and cost are critical. The semi-rigid RF connectors provide low VSWR with repeatable performance up to 26.5 GHz. The connectors have a stainless-steel body available with either passivated or gold finish. Termination type is soldered body with soldered separate center contact and the connectors are intermateable with 3.5 and 2.92 mm designs. The high-precision connectors meet all the performance requirements for MIL-PRF-39012 and the interface conforms to MIL-STD-348 FIG. 310. The Pisces waterproof series provides platforms available to be modified to create custom products. Full custom designs are welcomed with turnaround times typically of seven weeks. The company also manufactures a large range of coaxial adaptors, to facilitate interseries connection and gender change, etc., and connector and cable assemblies employing conventional cable and semi-rigid types including cryogenic semi-rigid cables for applications requiring operation at very low temperatures. Typical applications for the RF and waterproof connectors and cable assemblies include test and measurement, medical, marine, oil and gas, defense and general microwave markets. The new SMA RF Connectors are available from stock.

INTELLICONNECT USA

www.intelliconnectusa.com

Double-Balanced 2 - 14 GHz Mixer Features 24.4 dBm IIP3

THE LTC5549 double-balanced mixer from Linear Technology can operate either as an upconverter or downconverter with an RF frequency range from 2 to 14 GHz. The device features linearity of 24.4 dBm IIP3 at 9 GHz, an integrated LO buffer that needs only a 0 dBm drive level, and an integrated switchable frequency doubler for LO signal. A wideband integrated balun transformer is optimized to extend RF frequency bandwidth from 2 to 14 GHz while enabling single-ended operation. The IF port has wide bandwidth up to 6 GHz and all three ports are 50 Ω matched. High port-to-port isolation minimizes undesirable LO leakage and eases external filtering requirements. The mixer's performance enhances microwave applications including backhaul, high unlicensed band LTE-Advanced base stations, satellite broadband radios, radar systems, X-band and Ku band transceivers, test equipment and satellite modems.

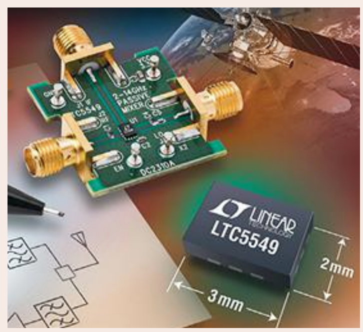

Rated for operation from –40°C to 105°C case temperature, the device is available in a 12-lead, 3 x 2 mm plastic QFN package and is optimized for single 3.3 V supply operation drawing 115 mA supply current. The LTC5549 double-balanced mixer is priced starting at $9.50 each/1,000 with samples and production quantities available immediately.

LINEAR TECHNOLOGY

www.linear.com

(continued from p. 31)

Figure 6 depicts SW1 gate drive pulse *T_on* time *(yellow line)* and rectified voltage *(green line)* at the input of the device. Rectified voltage drops slightly after the load is connected, due to the limited output power of the isolation transformer used during the test. The blue line depicts line current, while the red line depicts the load voltage. The system is verified to provide 2.5-A output current at full load at normal operation. Furthermore, inrush current is limited to 10 A.

Measured efficiency of the inrush control path is 99.5%. The device can work over a wide input voltage range of 80 to 240 V. Tested power-line frequency range was 50 Hz and 60 Hz; dedicated control pulse train was developed for each power-line frequency. In case of higher power-line voltage, a longer control pulse train is needed to keep the same amplitude of the inrush current. For instance, if the ac line voltage is 220 V, it requires a double pre-charging time to have the same peak inrush current when at 110 V.

Overload protection is based on continuous monitoring of the dynamic current from the bulk capacitor, In case of an overload condition, the current drawn from the capacitor instantly increases and the comparator inside the MCU initiates the system overload mode. Overload current threshold, number of overload instances, and the period between overload events are all programmable.

The system response was verified successfully by testing an overload condition. The load was increased to draw an output current of 3.5 A, which triggered an overload protection. The system was also tested with continuous overload, resulting in multiple attempts to restart the system with immediate interruption. Power Good status is not present in overload conditions. Overall, this overload protection isn't sensitive to power interruptions, brownout, and temperature variations.

CONCLUSION

IXYS's Digital Inrush Controller offers flexibility with its unique control algorithm, which aids in creating an efficient power system. Testing results revealed that the controller is able to achieve a high level of efficiency, increased stability, and reliable performance over a wide load range.

Thanks to an innovative current-measurement algorithm, the inrush controller allows for common input and load grounds. Users can optimize the device for a wide range of input voltages and frequencies. In addition, the design provides instant overcurrent protection, which is followed by an intervention by the microcontroller for corrective actions.

ANATOLIY TSYRGANOVICH, Fellow Systems Architect at Zilog (an IXYS division), holds Master's and PhD degrees in digital signal processing. Along with video and audio, his engineering field of expertise is in developing extreme efficiency of power converters via digital-control techniques. He is author of over 30 patents.

LEONID NEYMAN, Senior Application Manager at IXYS, holds a Master's degree in electromechanical engineering from Saint Petersburg State University of Aerospace Instrumentation, Russia, and Ph.D. degree in electronics engineering from Saint Petersburg State Electrotechnical University, Russia. His main engineering field is mixed analog/digital design, and is the author of 28 patents.

ABDUS SATTAR, Director of Engineering for power devices and applications at IXYS, holds an MS in engineering (electrical) from South Dakota State University, Brookings, and a PhD (electrical) from Santa Clara University, Calif. He is the author of several publications and patents in electron device physics. ed

REFERENCES

1. Randhir Singh Malik, William Hemena, Circuit for limiting inrush current to a power source, US6445165 B1, Sep 3, 2002.
2. Michael Allen, Understanding power supplies and inrush current, Electronic Products, March 2006, pp. 64, 65.

(continued from p. 25)

as needed, based on varying load conditions (plus coil alignment and coupling efficiency). There are two common approaches to varying output power: the TX coil can be excited with a constant-amplitude/variable frequency ac signal, or it can employ variable amplitude/fixed-frequency excitation.

Variable-frequency control eliminates the need for an adjustable pre-regulation stage on the TX side, and relies on the resonant tuning of the TX/RX tank circuits. When the TX operating frequency approaches the resonant point, the maximum possible power is transferred from the TX to the RX.

To reduce the power delivered to the RX side, the TX controller increases its frequency away from the resonant peak. At lighter loads (when the RX needs less power), there's a rise in TX frequency.

However, this approach makes the power delivery/control process dependent on coil characteristics. A variable-frequency architecture may also present some challenges in controlling electromagnetic interference (EMI) when used at higher power levels.

The 10-W transmitter system operates at fixed frequency, but implements an adjustable pre-regulator to vary the dc rail used for coil excitation. A full-bridge circuit will generate an ac excitation for the TX coil *(Fig. 3)*.

The 10-W wireless receiver output voltage can be adjusted with external feedback resistors across the 5- to 10-V range. This allows for charging of either one- or two-series cell configurations, and can maintain high efficiency for the one-cell case when combined with a wide-input-voltage-range, switch-mode, narrow-voltage direct-current (NVDC) type of charger. The NVDC charger architecture enables efficient charging of low-voltage batteries while reducing the input current required from a higher-voltage source (such as the wireless RX output).

RECEIVER CONSIDERATIONS

The thermal response of the receiver circuit is improved by using higher output voltage at lower current *(Fig. 4)*. Additionally, the series-resonant capacitor (C1) is critical in terms of optimizing thermal performance *(Fig. 5)*. In practice, multiple parallel capacitors are implemented to provide the total capacitance.

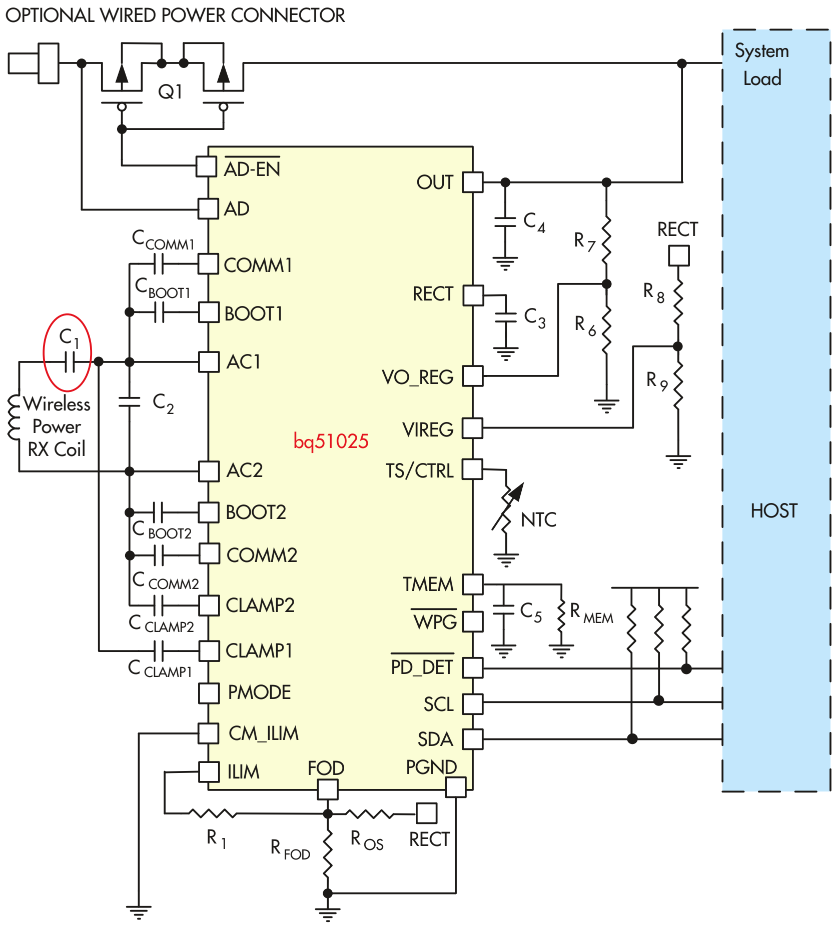

5. In a receiver circuit, the series-resonant capacitor (C1) is a critical component and is often implemented using multiple parallel capacitors.

REFERENCES:

Sengupta & Johns, "Universally compatible wireless power using the Qi protocol," *Low-Power Design*, October 1, 2011.

Tahar Allag, "Test and troubleshoot a wireless power receiver," Application Report (SLUA724), August 2014 Instruments.

Johns, Antonacci, and Siddabatula, "Designing a Qi-compliant receiver coil for wireless power systems," *Analog Applications Journal* (SLYT479), 3Q 2012.

Tahar Allag, "Layout Guidelines for wireless power receiver," Application Report (SLUA710), June 2014.

Ilya Kovarik, "Building a wireless power transmitter," Application Report (SLU-A635A), August 2012.

Jing Ye, "NVDC charging design considerations," Video Tutorial.

Norelis Medina, 10W Wireless power system lab demo, Video.

ABOUT THE AUTHORS

UPAL SENGUPTA is an applications manager with the Texas Instruments Battery Management Solutions group. He received a BSEE from the University of Illinois, and an MSEE from Michigan State University. For questions about this article, Upal can be contacted at ti_upalsengupta@list.ti.com.

DICK STACEY, an applications engineer in the Wireless and Low Power Charging team at Texas Instruments, has previously held roles in systems engineering, test engineering, and marketing for power-management products. He received his BSEE from the University of Texas at Austin.

BILL JOHNS, an applications engineer for Wireless Power at Texas Instruments, specializes in power conversion for portable battery-powered applications. He received his BSEE from University of Texas in Dallas.

Ad	Page

For more information on products or services visit our website **www.electronicdesign.com**, menu item Reader Service. The advertisers index is prepared as an extra service. *Electronic Design* does not assume any liability for omissions or errors.

BILL WONG | Embedded/Systems/Software Editor
bill.wong@penton.com

In This Martian Movie, They Get the Details Right

NASA gets on board to help make the new movie, "The Martian," as accurate as possible. The result is a great space adventure, one that could really happen.

Apollo 13 was the winner of sister publication *Machine Design*'s "World's Greatest Engineering Movie" because of its realism. The winner next time around just may be director Ridley Scott's new movie, *The Martian*, starring Matt Damon and Jessica Chastain. The movie follows the book of the same name by Andy Weir, a programmer and author, very closely.

1. In *The Martian*, astronaut Mark Watney (Matt Damon) has to grow his own food on Mars to survive.

Matt Damon plays NASA astronaut Mark Watney, who is on a mission to Mars that goes awry. The rest of the team thinks Watney is dead and heads back to earth in their ion-powered ship, but Watney is not dead. What ensues is a believable presentation of Watney's "MacGyver"-like ingenuity where he not only communicates with Earth but salvages, builds, and overcomes obstacles to move toward a rendezvous with a rescue mission. No big spoilers here.

I have heard a lot of people say that *Apollo 13* is fictionalized and it could never happen that way. Well, it did and it took a lot of work from a lot of people on the ground and in space. They tackled an amazing array of problems and came up with engineering solutions that worked.

While fiction, this new movie takes its science and engineering seriously. Watney has to make water and grow his own food (*Fig. 1*) because there are insufficient amounts of both to survive until a rescue arrives. We actually now know that Mars is a bit friendlier than in the movie because of soil testing that has revealed more water and nutrients in the soil than was known when the book was written.

NASA is already working on many of the items and concepts presented in the movie, from habitats to ion engines. Ridley Scott worked with Dr. Jim Green, director of the Planetary Science Division at NASA, to do the right stuff. Detailed designs for the movie's habitats and surface suits (*Fig. 2*) were completed prior to filming, as was the creation of the objects used in filming. Hacking *Pathfinder* and *Sojourner* in the movie is possible, as they are in the same area of Mars in which Damon is stranded—but *Curiosity* is on the other side of the planet.

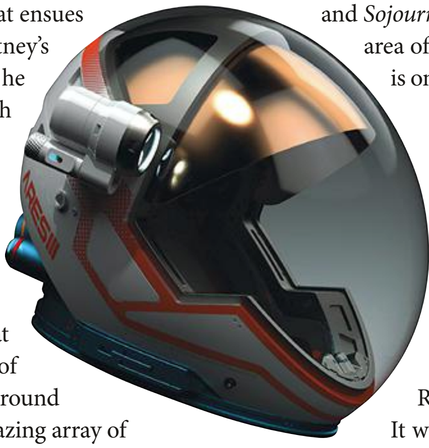

2. Director Ridley Scott worked closely with NASA in creating items like the Surface Suit helmet.

A few minor things are off. The first windstorm is a bit more turbulent than a real Martian windstorm would be, but the second is on par with those already recorded on Mars. This includes the lightning. Likewise, Watney would probably not dig up the Multi-Mission Radioisotope Thermoelectric Generator (MMRTG). It would not have been buried because it would have human microbes on it that could grow in the Martian soil. NASA does use MMRTGs, but they would be kept above ground so a more realistic chore would be traveling to a remote location where the MMRTG would be powering some device.

I am definitely looking forward to seeing *The Martian*. ed

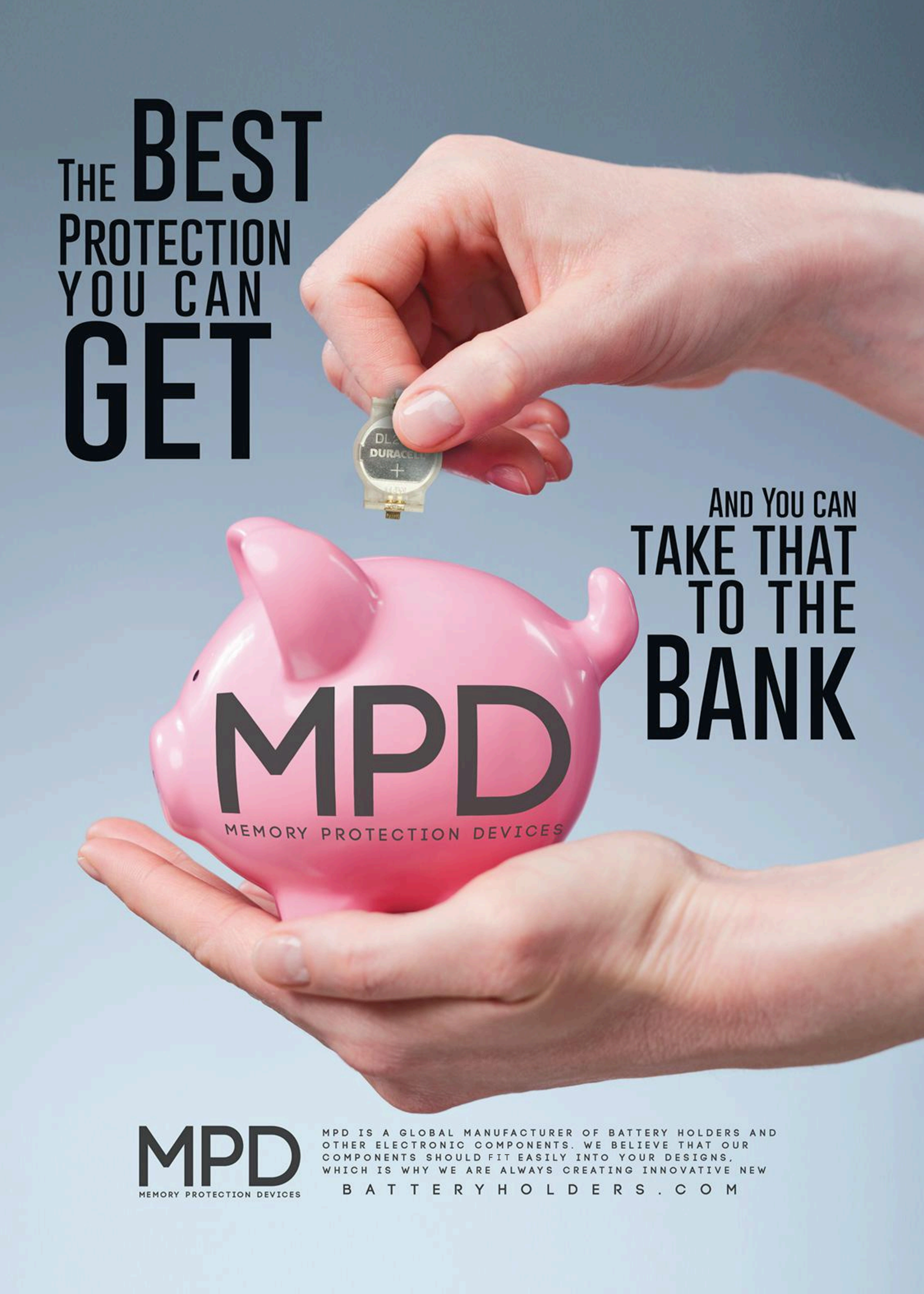

The BEST
Protection
you can
GET
And You can
take that
to the
Bank
MPD
MEMORY PROTECTION DEVICES
MPD
MEMORY PROTECTION DEVICES
MPD IS A GLOBAL MANUFACTURER OF BATTERY HOLDERS AND OTHER ELECTRONIC COMPONENTS. WE BELIEVE THAT OUR COMPONENTS SHOULD FIT EASILY INTO YOUR DESIGNS, WHICH IS WHY WE ARE ALWAYS CREATING INNOVATIVE NEW
BATTERYHOLDERS.COM

35V Buck Battery Charger with Digital Telemetry

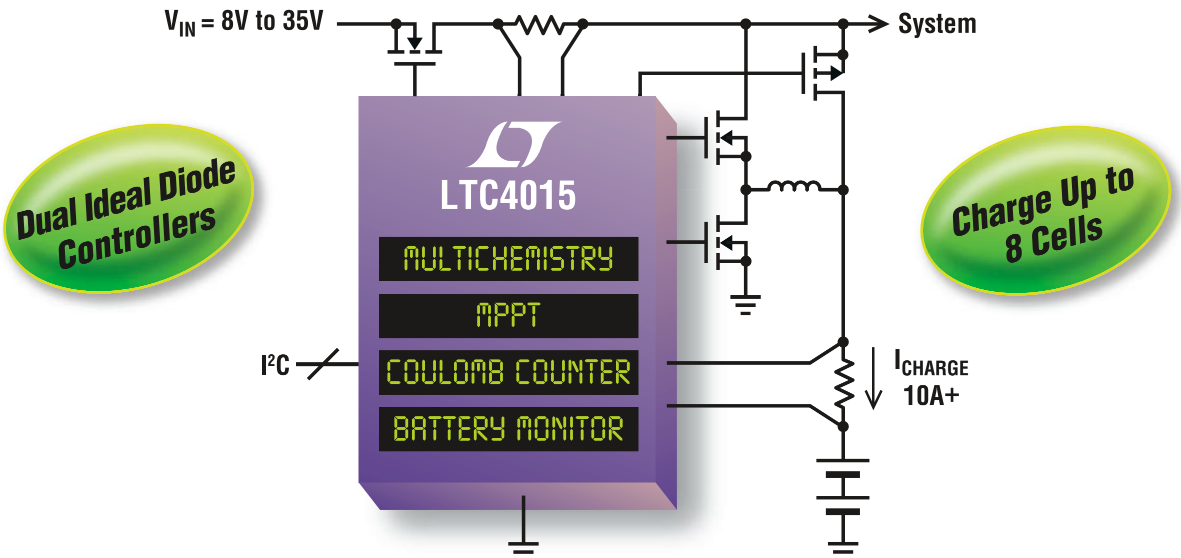

Multichemistry, Coulomb Counter & Battery Health Monitoring

The LTC®4015 is a complete synchronous buck controller/charger for single or multiple Li-Ion/Polymer, $LiFePO_4$ or lead-acid battery chemistries with on-chip termination algorithms. Many system parameters can be programmed and/or digitally monitored, including battery voltage and current, battery series resistance, input voltage & current plus battery & die temperatures, all via an I²C port. Battery health can be tracked with the battery series resistance measurement and integrated coulomb counter. The LTC4015 also supports stand-alone applications with no digital programming required.

Features

- Multichemistry Charger with Termination
- High Efficiency Synchronous Buck Topology
- Input Voltage Range: 4.5V to 35V
- Digital Telemetry System Monitors for Most Parameters
- Coulomb Counter and 14-Bit ADC
- PowerPath™ Control for Instant-on Operation
- Maximum Power Point Tracking

Charger Efficiency & Coulomb Counter Error vs. Charge Current

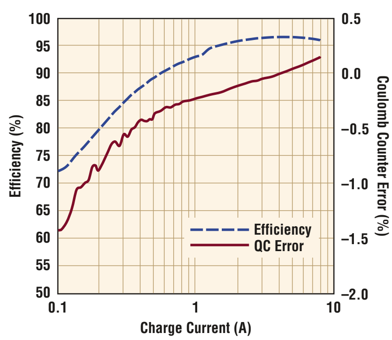

Info & Free Samples

www.linear.com/product/LTC4015

1-800-4-LINEAR

Free Battery Charger Solutions Brochure

www.linear.com/batsolutions